

## A WIDE-FIELD SURVEY OF TWO $z \sim 0.5$ GALAXY CLUSTERS: IDENTIFYING THE PHYSICAL PROCESSES RESPONSIBLE FOR THE OBSERVED TRANSFORMATION OF SPIRALS INTO S0s

SEAN M. MORAN,<sup>1</sup> RICHARD S. ELLIS,<sup>1</sup> TOMMASO TREU,<sup>2,3</sup> GRAHAM P. SMITH,<sup>4</sup> R. MICHAEL RICH,<sup>5</sup> AND IAN SMAIL<sup>6</sup>

Received 2007 June 29; accepted 2007 July 26

### ABSTRACT

We present new results from our comparative survey of two massive, intermediate-redshift galaxy clusters, Cl 0024+17 ( $z = 0.39$ ) and MS 0451–03 ( $z = 0.54$ ). Combining optical and UV imaging with spectroscopy of member galaxies, we identify and study several key classes of “transition objects” whose stellar populations or dynamical states indicate a recent change in morphology and star formation rate. For the first time, we have been able to conclusively identify spiral galaxies in the process of transforming into S0 galaxies. This has been accomplished by locating both spirals whose star formation is being quenched and their eventual successors, the recently created S0s. Differences between the two clusters in both the timescales and spatial location of this conversion process allow us to evaluate the relative importance of several proposed physical mechanisms that could be responsible for the transformation. Combined with other diagnostics that are sensitive to either ICM-driven galaxy evolution or galaxy-galaxy interactions, we describe a self-consistent picture of galaxy evolution in clusters. We find that spiral galaxies within infalling groups have already begun a slow process of conversion into S0s, likely via gentle galaxy-galaxy interactions. The fates of spirals upon reaching the core of the cluster depend heavily on the cluster ICM, with rapid conversion of all remaining spirals into S0s via ram pressure stripping in clusters where the ICM is dense. In the presence of a less dense ICM, the conversion continues at a slower pace, with other mechanisms continuing to play a role. We conclude that the buildup of the local S0 population through the transformation of spiral galaxies is a heterogeneous process that nevertheless proceeds robustly across a variety of different environments.

*Subject headings:* galaxies: clusters: individual (Cl 0024+1654, MS 0451–0305) — galaxies: elliptical and lenticular, cD — galaxies: evolution — galaxies: spiral — galaxies: stellar content — ultraviolet: galaxies

*Online material:* color figures, machine-readable tables

### 1. INTRODUCTION

It is well known that environmental processes play a significant role in shaping the evolution of galaxies as they assemble onto clusters. With the aid of *Hubble Space Telescope* (*HST*) imaging and deep optical spectroscopy, recent studies have quantified this evolution in galaxy properties, painting a picture where the fraction of early-type (elliptical and S0) galaxies and the fraction of passive non–star-forming galaxies both grow with time, and at a rate that seems to depend sensitively on the local density of galaxies (Dressler et al. 1997; Poggianti et al. 1999; Smith et al. 2005a; Postman et al. 2005).

Yet there are a wide variety of physical processes that may be responsible for these evolutionary trends, including galaxy mergers, galaxy-galaxy harassment, gas stripping by the ICM, or tidal processes (Moore et al. 1999; Fujita 1998; Bekki et al. 2002). Observationally, it has so far been impossible to fully separate the effects of the various physical processes, in large part due to the overlapping regimes of influence for each of the proposed mechanisms (see Treu et al. 2003, hereafter Paper I). Further complicating the picture, the large-scale assembly states of clusters show considerable variety (Smith et al. 2005b), such that the dominant forces acting on galaxies are likely to vary from cluster to cluster, or over the course of an individual cluster’s assembly history.

But gaining an understanding of the complex interplay between a variable ICM, the properties of assembling galaxies, and the overall cluster dynamical state is crucial if we are to have a complete picture of the growth and evolution of galaxies in a hierarchical universe.

In this paper we combine optical (*HST*) and UV (*GALEX*) imaging of two  $z \sim 0.5$  galaxy clusters with ground-based spectroscopy of member galaxies, in an attempt to trace directly the buildup of passive early-type galaxies via a detailed “case study” of the galaxy population across each cluster. The two studied clusters, Cl 0024+17 ( $z = 0.40$ ) and MS 0451 ( $z = 0.54$ ), are part of a long-term campaign to trace the evolution of galaxies in wide fields ( $\sim 10$  Mpc diameter) centered on both clusters, using a variety of methods. By undertaking an in-depth, wide-field comparative study of two prominent clusters, we hope to provide a complement to other observational (e.g., Cooper et al. 2007; Poggianti et al. 2006) and theoretical investigations (e.g., de Lucia et al. 2006) that trace with a broad brush the evolution in star formation rate (SFR) and the buildup of structure in the universe.

The first paper in our series, Paper I, introduced our panoramic *HST* imaging of Cl 0024 and began our ongoing discussion of the physical processes that may be acting on galaxies within clusters. In several subsequent papers, whose results are summarized in § 2, we have added extensive optical spectroscopy to the program, allowing targeted investigations of galaxy stellar populations and SFRs as a function of clustercentric radius, local density, and morphology. Our goal for this paper is to bring our complete survey data set to bear on the question of how galaxies are affected by their environment, as a function of both the overall cluster properties and the local environment within each cluster. For maximum clarity and deductive power, we focus our investigation on

<sup>1</sup> Department of Astronomy, California Institute of Technology, MS 105-24, Pasadena, CA 91125; smm@astro.caltech.edu, rse@astro.caltech.edu.

<sup>2</sup> Department of Physics, University of California, Santa Barbara, CA 93106; tt@physics.ucsb.edu.

<sup>3</sup> Alfred P. Sloan Research Fellow.

<sup>4</sup> School of Physics and Astronomy, University of Birmingham, Edgbaston, Birmingham B15 2TT, UK.

<sup>5</sup> Department of Physics and Astronomy, UCLA, Los Angeles, CA 90095.

<sup>6</sup> Institute for Computational Cosmology, Durham University, Durham DH1 3LE, UK.

TABLE 1  
BASIC PROPERTIES OF THE CLUSTERS

Name	R.A. (deg)	Decl. (deg)	$R_{\text{vir}}$ (Mpc)	$M_{200}$ ( $M_{\odot}$ )	$z$	$L_X$ ( $L_{\odot}$ )	$T_X$ (keV)
Cl 0024 .....	6.65125	17.162778	1.7 <sup>a</sup>	$8.7 \times 10^{14b}$	0.395	$7.6 \times 10^{10c}$	3.5 <sup>c</sup>
MS 0451 .....	73.545417	-3.018611	2.6	$1.4 \times 10^{15d}$	0.540	$5.3 \times 10^{11d}$	10.0 <sup>d</sup>

<sup>a</sup> Paper I.

<sup>b</sup> Paper II.

<sup>c</sup> Zhang et al. (2005).

<sup>d</sup> Donahue et al. (2003).

several key populations of “transition galaxies” in the clusters, galaxies whose stellar populations or dynamical states indicate a recent or ongoing change in morphology or SFR.

In evaluating cluster galaxies for signs of evolution, we have adopted a strategy to make maximal use of our *HST*-based morphologies by characterizing signs of recent evolution in spirals and early types separately. This approach is similar to using the color-magnitude relation to divide our sample into “red sequence” and “blue cloud” galaxies, but it provides additional leverage to identify galaxies in transition. Early-type galaxies that have been either newly transformed or prodded back into an active phase or spiral galaxies where star formation is being suppressed or enhanced will all stand out in our sample. At the same time, their morphologies reveal important information about their formation histories prior to their current transition state, information that colors alone do not provide. Our strategy also has the benefit of allowing us to directly investigate the hypothesis that many cluster spirals transform into S0s between  $z \sim 0.5$  and today (Dressler et al. 1997), an investigation that will form the basis of this paper.

In the next section we outline our rationale for selecting Cl 0024 and MS 0451, describe the large-scale properties of each cluster, and give a summary of what we have concluded so far in our study of galaxy evolution in both clusters. In § 3 we describe new data not covered in previous papers in our series. In § 4 we investigate the properties of “passive spirals” across the two clusters, suggesting that they are in the process of transforming into S0 galaxies. We confirm in § 5 that this is the case, via identification of newly created S0s that we believe reflect the distinct passive spiral populations found in each cluster. In § 6 we consider the environments of these galaxies in transition and begin to investigate the physical mechanisms that may be responsible for these transformations. In § 7 we outline a model of how galaxy evolution proceeds in each cluster. We consider the fundamental plane (FP) as a way to further constrain the physical mechanisms at work and derive similar constraints from the populations of compact emission-line galaxies in both clusters. Finally, in § 8 we summarize our conclusions about the transformation of spirals into S0s at  $z \sim 0.5$ . In this paper we adopt a standard  $\Lambda$ CDM cosmology with  $H_0 = 70 \text{ km s}^{-1} \text{ Mpc}^{-1}$ ,  $\Omega_m = 0.3$ , and  $\Omega_{\Lambda} = 0.7$ .

## 2. A COMPARATIVE SURVEY OF TWO $z \sim 0.5$ CLUSTERS

Cl 0024 and MS 0451 were chosen for study primarily because of their comparable total masses, similar galaxy richness, and strong-lensing features, while exhibiting X-ray properties that are quite distinct (see Table 1). While MS 0451 is one of the most X-ray-luminous clusters known (Donahue et al. 2003), Cl 0024 is somewhat underluminous in the X-ray, with a mass inferred from *XMM-Newton* observations that significantly underestimates the

mass derived from other methods (Zhang et al. 2005). MS 0451 has X-ray luminosity 7 times larger than Cl 0024, with a corresponding gas temperature nearly 3 times as high. This implies a large difference in the density and radial extent of the intracluster medium (ICM) between the two clusters. As a result, ICM-related physical processes are naively expected to be more important in the evolution of currently infalling MS 0451 galaxies than in Cl 0024.

In the schematic diagram shown in Figure 1, we apply simple scaling relations to estimate the regimes of influence for several key physical processes that could be acting on infalling galaxies, following the procedure described in Paper I. ICM-related processes, such as gas starvation (Larson et al. 1980; Bekki et al. 2002) and ram pressure stripping (Gunn & Gott 1972), begin to affect galaxies at much larger radius in MS 0451. As in Paper I, we expect that other ICM-related processes such as thermal evaporation (Cowie & Songaila 1977) or viscous stripping (Nulsen

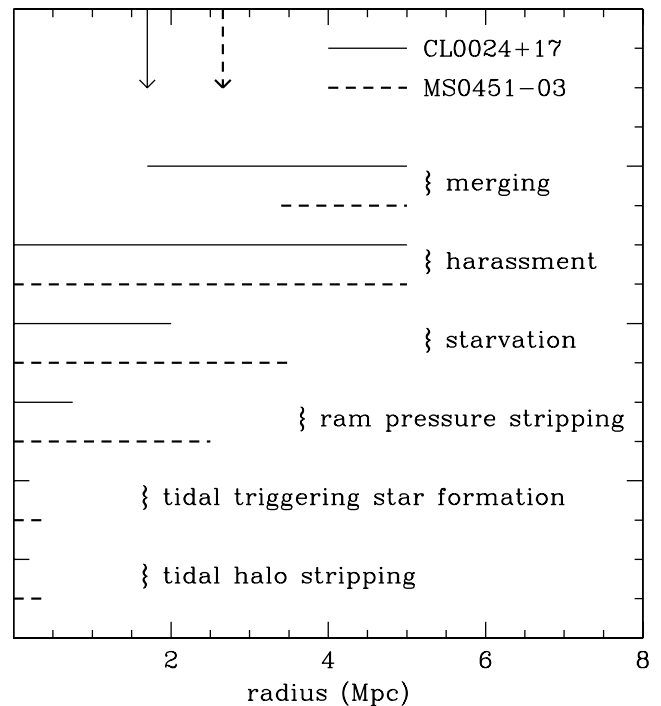


FIG. 1.—Schematic diagram indicating the clustercentric radius over which each of several listed physical mechanisms may be effective at fully halting star formation or transforming the visual morphology of a radially infalling galaxy. Each physical mechanism listed can act effectively over the radial range indicated by the solid (Cl 0024) or dashed line (MS 0451). Arrows indicate the virial radius for each cluster. Note that tidal processes here refer to interactions with the cluster potential, while tidal forces during galaxy-galaxy interactions are a component of the harassment mechanism. Each regime of influence was calculated according to the simple models described in Paper I for Cl 0024, using the global cluster properties given in Table 1.

1982) operate with at most similar strength to ram pressure, and so we do not consider them separately. An important caveat, however, is that the role of difficult-to-observe shocks in the ICM is unknown and is not accounted for in Figure 1 (but see § 7). Similarly, the two clusters' differing masses set the radial regions where galaxy merging will be effective; because of the  $\sim 50\%$  higher mass of MS 0451, typical galaxy relative velocities become too fast for mergers to occur at a higher radius than in Cl 0024.

The differing regimes of influence for the physical mechanisms illustrated in Figure 1 provide the key template for our attempt to disentangle the relative importance of the various processes. By surveying the galaxies of both clusters for signs of recent transformation or disturbance, across the entire radial range to  $\sim 5$  Mpc, we hope to associate the sites and characteristics of galaxies in transition with the likely causes from Figure 1.

An additional factor not reflected in Figure 1, however, is the overall assembly state and level of substructure in each cluster. Therefore, Figure 1 can only be used as a guide, and we must carefully consider the effects that large-scale cluster assembly and irregularities may have on their galaxies as well. For example, the effects of tidal processes and galaxy-galaxy harassment, which according to Figure 1 should occur in much the same regions across both clusters, may very well differ greatly between clusters depending on how well each is virialized. As we discuss below, there are marked differences in the levels of substructure between the two clusters, and these may drive important differences between the galaxy populations.

### 2.1. Kinematic Structure of the Two Clusters

While it is evident from their different X-ray luminosities that MS 0451 and Cl 0024 provide quite different environments for their constituent galaxies, our detailed study of environmental effects on cluster galaxies requires a comprehensive characterization of the two clusters and their respective environments. Here we study the radial velocities and spatial distributions of galaxies in each cluster, in order to evaluate the global kinematic structure of each cluster and identify significant substructures.

Our extensive *HST* imaging and Keck spectroscopy, which are described more fully in § 3, readily reveal marked differences in the distributions of galaxies between the two clusters, suggesting that the clusters have quite dissimilar recent assembly histories. In Figure 2 we display the distribution of redshifts for members of both Cl 0024 and MS 0451. The redshift distribution of MS 0451 members is broadly consistent with a Gaussian distribution. A somewhat better fit to the data is given by a two-component double-Gaussian function, but the distribution splits into these two peaks only for galaxies at large radius ( $R > 2$  Mpc), suggesting that we are observing two filaments feeding galaxies into the virialized center of MS 0451. Cl 0024 galaxies likewise exhibit a double-peaked structure in redshift space, with two components that are widely separated and asymmetric in height. This feature was discovered by Czoske et al. (2001) and is thought to be the remnant of a high-speed, face-on encounter between the main cluster and a smaller subcluster or large group (Czoske et al. 2002).

The effects of this collision, even an estimated several billion years after it occurred (Czoske et al. 2002), are still important in the core of Cl 0024, for example, as shown by intriguing recent claims of a “dark matter ring” in the core of Cl 0024 (Jee et al. 2007). The measured line-of-sight velocity dispersion in the core of  $650 \pm 50$  km s $^{-1}$  implies a 30%–50% lower mass than has been directly measured through strong- and weak-lensing constraints (Kneib et al. 2003, hereafter Paper II). The fact that the

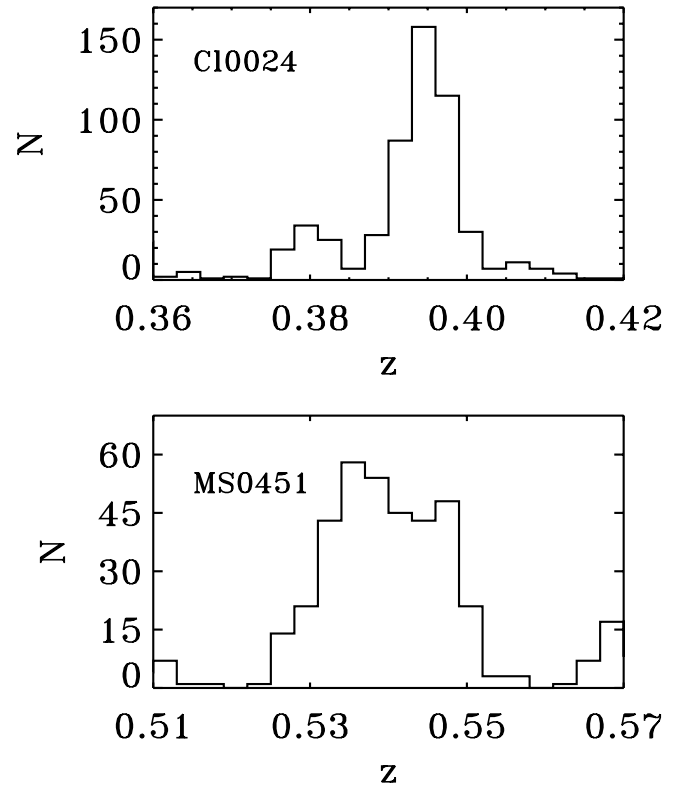


FIG. 2.—Distribution of redshifts for both Cl 0024 (*top*) and MS 0451 (*bottom*), including all galaxies with spectroscopically confirmed redshifts from our observations, as well as previously published redshifts (see § 3). In Cl 0024, we identify 508 cluster members, defined to lie in the range  $0.373 < z < 0.402$ . In MS 0451, we count 319 cluster members in the range  $0.52 < z < 0.56$ .

galaxy velocity distribution and X-ray-emitting gas both underestimate the mass leads to the conclusion that the core of Cl 0024 is not in virial or hydrostatic equilibrium, an assumption that was made for each of these mass estimates. The lower relative velocities of galaxies in the Cl 0024 core may importantly affect the action of physical processes whose strengths vary with galaxy velocity. For example, gas stripping by the ICM may be even less effective in Cl 0024 than naively predicted by Figure 1. The effects of galaxy-galaxy harassment may also be different, as close galaxy encounters may happen at both lower frequency and lower relative velocities than have previously been modeled in detail (e.g., Moore et al. 1999).

The spatial distributions of galaxies in MS 0451 and Cl 0024 also show key differences. In Figure 3 we construct modified Dressler-Shectman (D-S) plots for the region within  $R_V$  of each cluster (Dressler & Shectman 1988). In such plots, each cluster member is indicated by a circle, with the size of the circle proportional to that galaxy’s “Dressler-Shectman statistic:”

$$\delta^2 = \frac{11}{\sigma^2} \left[ (\bar{v}_{\text{local}} - \bar{v})^2 + (\sigma_{\text{local}} - \sigma)^2 \right], \quad (1)$$

where line-of-sight velocity  $\bar{v}_{\text{local}}$  and dispersion  $\sigma_{\text{local}}$  are measured with respect to each galaxy’s 10 nearest neighbors, and  $\bar{v}$  and  $\sigma$  are the global cluster values. This statistic measures each galaxy’s local deviation from a smooth, virialized velocity and spatial distribution. In other words, groups of large circles on the plot tend to indicate the presence of an infalling group. In Figure 3 we further color-code each galaxy according to its velocity with respect to the cluster center.

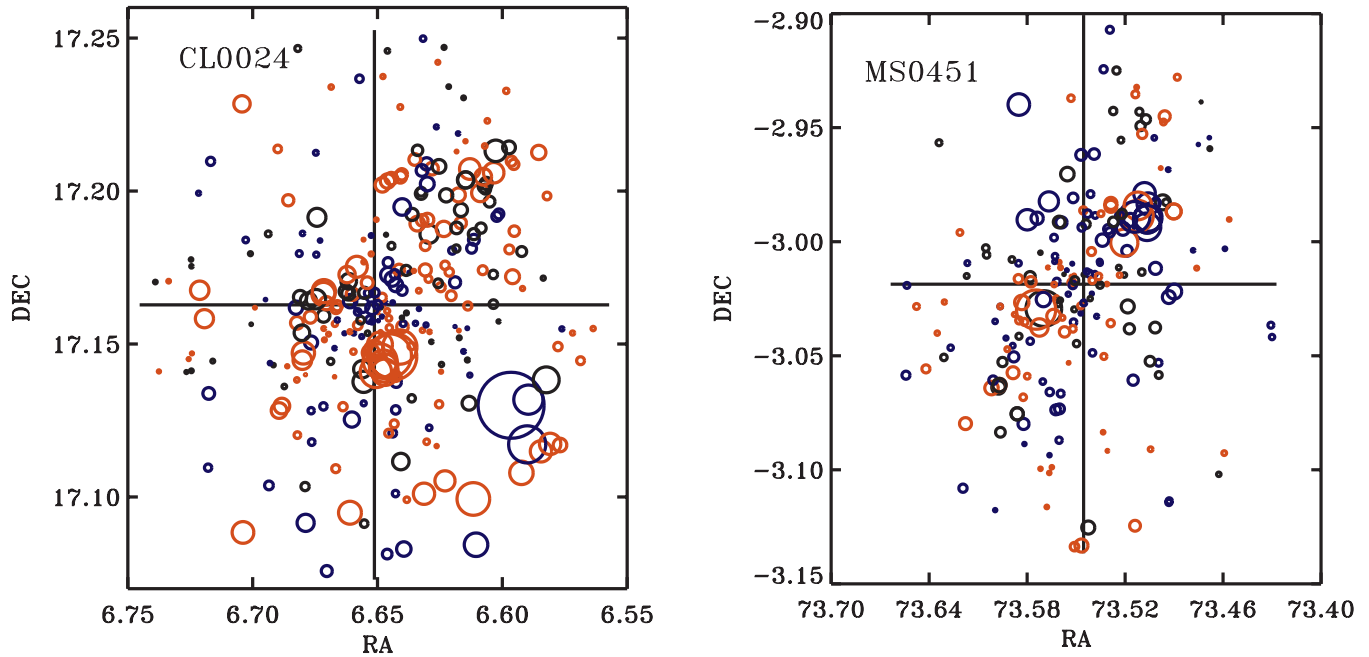


FIG. 3.—Dressler-Shectman plots for Cl 0024 (*left*) and MS 0451 (*right*). Including only spectroscopically confirmed objects within  $1R_V$  of the cluster center, each circle indicates the spatial position of a cluster member, with the circle size proportional to its local deviation from a smooth velocity distribution (see text). Circles are coded blue for galaxies with clustercentric velocity toward the observer with amplitude  $>300 \text{ km s}^{-1}$ , red for galaxies with the same velocity amplitude away from the observer, and black for galaxies with low clustercentric velocities,  $<300 \text{ km s}^{-1}$ .

The D-S plot for Cl 0024 reveals the presence of at least two significant groups near to the cluster core: an infalling group at high velocity nearly along the line of sight to the cluster center, and a previously noted large group to the northwest of the cluster core, presumably assembling onto the core in an orientation almost in the plane of the sky. The large structure to the northwest is also detected in both the weak-lensing map (Paper II) and *XMM-Newton* observations (Zhang et al. 2005), which additionally suggest the presence of a shock front at the interface between the group and the main cluster.

In contrast, the D-S plot for MS 0451 reveals an elongated but largely smooth distribution of galaxies. The cluster’s elliptical shape is clearly visible, but the segregation of red points to the southeast and blue points to the northwest suggests a uniform contraction of the cluster along its major axis. While it is possible that the observed velocity field is due to cluster-scale rotation, previous analyses of the X-ray and Sunyaev-Zel’dovich observations prefer a prolate or triaxial shape for MS 0451 (Donahue et al. 2003; De Filippis et al. 2005), whereas the cluster would necessarily be oblate if the observed velocities are due to rotation. We may be seeing this spread in velocities reflected in the redshift distribution of MS 0451, which splits into two peaks at large radius, likely indicating infall from two directions. One might worry that the elongated distribution gives MS 0451 an artificially large velocity dispersion,  $\sigma$ , but cluster mass estimates derived from  $\sigma$  are consistent with those derived from the X-ray and weak-lensing analysis (Donahue et al. 2003 and references therein). The origin of the elliptical shape is unclear but may represent the remnant of a past major merger. Nevertheless, still-bound infalling groups appear to be absent or insignificant within the virial radius.

The overall increased level of substructure observed in Cl 0024 is likely to have implications for the galaxy population. In comparison to MS 0451, Cl 0024 galaxies are more likely to have been a member of an infalling group in the recent past, and so we may expect to see more signs of recent group “preprocessing” in

Cl 0024. Furthermore, in the chaotic environment of Cl 0024 the ICM is more likely to be disturbed, and so shocks, cold fronts, or other features in the ICM may be present and could play an important role in the star formation histories of cluster members (Roettiger et al. 1996).

## 2.2. Previous Work

Between the extremely dense ICM in MS 0451 and the active assembly state of Cl 0024, these two clusters provide very distinct environments for their member galaxies. In the course of this paper we examine how the properties of transition galaxies in each cluster reflect these distinct environments. However, as our new results rely on and incorporate the findings of our previous papers in this series, we present here a brief summary of our investigations so far. We highlight in particular several results that, in the initial interpretation, hint at the action of one or more physical mechanisms from Figure 1:

1. By constructing the FP of Cl 0024, we observed in Moran et al. (2005, hereafter Paper III) that elliptical and S0 galaxies (E+S0s) exhibit a high scatter in their FP residuals, equivalent to a spread of 40% in mass-to-light ratio ( $M/L_V$ ). The high scatter occurs only among galaxies in the cluster core, suggesting a turbulent assembly history for cluster early types, perhaps related to the recent cluster-subcluster merger (Czoske et al. 2002).

2. Around the virial radius of Cl 0024, we observed a number of compact, intermediate-mass ellipticals undergoing a burst of star formation or weak active galactic nucleus (AGN) activity, indicated by strong [O II] emission (Paper III). The [O II] emitters reside in relatively low density and high speed regions, and so we deemed that they are not likely the remnants of mergers. Although we revisit the merger hypothesis in § 7, we tentatively conclude that the observed activity is caused by a rapidly acting physical process: two candidates are galaxy harassment and shocks in the ICM, perhaps generated by the subcluster merger in Cl 0024.

3. We searched for disruptions in the internal structures and SFRs of disk galaxies due to tidal effects or galaxy-galaxy interactions, by measuring emission-line rotation curves and constructing the Tully-Fisher (TF) relation (Moran et al. 2007). We find that the cluster TF relation exhibits significantly higher scatter than the field relation, echoing the high scatter seen in the C1 0024 FP. We argue that the high scatter in both  $K$ - and  $V$ -band TF relations demonstrates that cluster spirals are kinematically disturbed by their environment. We proposed that such disturbances may be due to galaxy merging and/or harassment.

4. We combined *GALEX* UV observations with key spectral line indices to place strict constraints on the recent star formation histories of passive spiral galaxies, an important class of transition object (Moran et al. 2006). Passive spirals show spiral morphology in *HST* images but reveal weak or no [O II] emission in their spectra, suggesting a lack of current star formation. Through *GALEX* UV imaging, we find that passive spirals in C1 0024 exhibit UV emission nearly as strong as regular star-forming spirals, implying the presence of young stars. Their unusual combination of UV emission with weak  $H\delta$  strength supports a picture where passive spirals have experienced a rapid decline and eventual cessation of star formation over the last  $\sim 0.5$ – $2$  Gyr. The time-scale of this decline suggests “starvation” by the ICM as a possible cause (Larson et al. 1980; Bekki et al. 2002), a process where the ICM strips gas from a galaxy’s halo, causing star formation to decline due to the absence of new cold gas accretion onto the disk.

Each of these previous investigations has revealed a partial view of environmental evolution across the studied clusters. Through these investigations, we have identified several physical mechanisms that we could call “likely suspects” for driving galaxy evolution in clusters, and these seem to fall into two classes: galaxy-ICM interactions and galaxy-galaxy interactions. However, a unified picture is still lacking. Both of these flavors of interaction have been implicated before in the decline of star formation and the possible conversion of spirals into S0s (see Boselli & Gavazzi 2006 and references therein), yet a detailed evaluation of their importance remains elusive.

We aim in this paper to complete our accounting of galaxy evolution across these two quite distinct clusters, building on and linking our earlier work into what we hope will be a more comprehensive picture of how cluster galaxies are affected by their environment at intermediate redshift. To accomplish this, we first document what we believe to be direct evidence for the transformation of spirals into S0s: through an analysis of their stellar populations and recent SFRs, we link the passive spiral galaxies in both clusters to their eventual end states as newly generated cluster S0 galaxies. Only then, as we examine the physical mechanisms responsible for this transformation, will we draw on the above-summarized results to place extra constraints on the physics driving the transformation. This discussion includes an extension of our analysis of the FP and the strongly emitting compact E+S0s in C1 0024 to include MS 0451, in order to further strengthen the constraints we can place on galaxy-galaxy interactions and galaxy-ICM interactions, respectively.

### 3. NEW DATA

Before turning to our new analysis, we must specify the characteristics of our now complete data set. While most imaging and spectroscopic data on C1 0024 have been fully or partially described in previous papers (Moran et al. 2006; Papers I and III), much of the following relies on new data for MS 0451. In this section we describe our new observations of MS 0451 and pro-

vide updated information on C1 0024, including *GALEX* imaging and additional spectroscopy.

#### 3.1. Imaging

We make use of *HST* imaging of C1 0024 and MS 0451 from the comprehensive wide-field survey described in Paper I and G. P. Smith et al. (2008, in preparation). In C1 0024, *HST* coverage consists of a sparsely sampled mosaic of 39 WFPC2 images taken in the F814W filter ( $\sim I$  band), providing coverage to a projected radius  $>5$  Mpc at exposure times of 4–4.4 ks. MS 0451 observations were taken with the Advanced Camera for Surveys (ACS), also in F814W, and provide contiguous coverage within a 10 Mpc  $\times$  10 Mpc box centered on the cluster, with single-orbit (2 ks) depth over the field.

For both clusters, reliable morphological classification is possible to rest-frame absolute magnitude  $M_V = -19.5$ , corresponding to  $I = 22.1$  in MS 0451 and  $I = 21.2$  in C1 0024. Broader classification as early or late type is possible to a fainter limit,  $M_V = -18.0$ . All galaxies that have spectroscopically confirmed redshifts and are brighter than this limit are classified visually following the procedure described in Paper I for C1 0024. In MS 0451, galaxies were classified by one of us (R. S. E.), and we expect that the typing is accurate to the quoted limits based on previous experience with ACS imaging of similar depth (e.g., Treu et al. 2005). Morphologies were assigned according to the Medium Deep Survey scheme introduced by Abraham et al. (1996): T =  $-2$  = star,  $-1$  = compact, 0 = E, 1 = E/S0, 2 = S0, 3 = Sa + b, 4 = S, 5 = Sc + d, 6 = Irr, 7 = Unclass, 8 = Merger, 9 = Fault. In the following, all galaxies assigned types T = 0, 1, 2 are together labeled as “early types” or E+S0s, and all galaxies with T = 3, 4, 5 are labeled as spirals.

C1 0024 and MS 0451 were observed for 15 and 80 ks, respectively, with *GALEX* (Martin et al. 2005) in 2004 October (GO-22; Cycle 1; PI: Treu), reaching comparable depths in rest-frame far-ultraviolet (FUV) (observed near-ultraviolet [NUV]). Galaxy fluxes were measured within  $6''$  circular apertures, centered on the optical position, on images reduced and sky subtracted using the standard automated *GALEX* reduction pipeline. The aperture size is chosen to be comparable to the measured NUV FWHM ( $5.5''$ ) to avoid difficulty with source confusion, which can be a significant issue for *GALEX* imaging. This problem limits our ability to measure total fluxes in larger ( $>6''$ ) apertures centered on the optical position, as contamination from nearby sources becomes much higher. As a result, we apply an aperture correction to bring our aperture fluxes into agreement with SExtractor-derived total magnitudes (MAG\_AUTO), and for comparison to MAG\_AUTO magnitudes in F814W (Bertin & Arnouts 1996). We note that at the redshifts of the clusters, most galaxies are effectively point sources at *GALEX* resolution, so we do not expect that the aperture corrections introduce significant errors into the photometry.

While observed F814W provides a good match to rest-frame  $V$  for both C1 0024 and MS 0451, we also make use of supplemental ground-based imaging to aid in determining  $k$ -corrections to transform observed magnitudes to the nearest rest-frame bands. Ground-based data include panoramic  $K_s$  band imaging of both clusters, along with  $J$ -band imaging of C1 0024, obtained with the WIRC camera on the Hale 200" telescope at Palomar Observatory (Wilson et al. 2003). These near-infrared data are supplemented with optical imaging in  $BVR$ I bands from either the 3.6 m Canada-France-Hawaii Telescope (CFHT; C1 0024) or the Subaru 8 m telescope (MS 0451), which have been described in Moran et al. (2007).

We use the Kcorrect software v.4\_1\_2 (Blanton et al. 2003) to estimate the necessary  $k$ -corrections; we make use of imaging

in all available bands from NUV to  $K_s$ , modeling each galaxy's spectral energy distribution and deriving the best-fit correction on a galaxy-by-galaxy basis. However, we find that the derived  $k$ -correction is mostly insensitive to the omission of one or several bands, with scatter typically  $\sim 0.1$  mag. We assume a Galactic extinction of  $E(B - V) = 0.056$  for Cl 0024 and 0.033 for MS 0451 (Schlegel et al. 1998), and all absolute magnitudes are expressed on the AB system.

We note also that, in all cases where we quote rest-frame colors, we have applied a  $k$ -correction equal to the *median*  $k$ -correction for all galaxies of the same morphological type and in the same cluster, rather than the individually fitted  $k$ -corrections. We do this to avoid introducing any additional scatter into the rest-frame colors (due to uncertainties in the  $k$ -corrections), above that present in the observed-frame colors. In general, the difference between the two methods is  $< 0.1$  mag, and we do not expect the method of  $k$ -correction to impact our analysis significantly.

### 3.2. Spectroscopy

We have used DEIMOS on Keck II to obtain deep spectra of  $\sim 1500$  galaxies per cluster in the fields of Cl 0024 and MS 0451. In both clusters, we observe with  $1''$  wide slits with lengths much larger than the galaxy size (typically  $8'' - 12''$ ). For each cluster, spectral setups were chosen to span rest-frame wavelengths from  $\sim 3500$  to  $\sim 6700$  Å, covering optical emission lines [O II], [O III], H $\beta$ , and, more rarely, H $\alpha$ .

Observations of Cl 0024 from 2001 October to 2003 October are described in Papers I and III. Integrations totaled 2.5 hr per mask, and targets were selected from the CFHT  $I$ -band mosaic, with priority given to known cluster members with *HST* morphologies, followed by galaxies in the *HST* survey without a known redshift, to  $I < 22.5$ .

We undertook an initial redshift survey of MS 0451 during 2003 October, observing 14 slit masks for 1 hr each, with the 600 line  $\text{mm}^{-1}$  grating set to central wavelength 7500 Å. This allowed redshift identification for 1300 objects, including 250 cluster members. Targets were selected from the  $I$ -band Subaru image, as the ACS mosaic was not yet available. We first selected objects randomly from the set with  $I < 21.5$  and then filled in slit mask gaps with fainter objects ( $I < 23.0$ ).

We have additionally observed both clusters again in 2004 December and 2005 October. For the 2004 December run, spectroscopic targets in Cl 0024 were selected in the same manner as previous runs. Integrations were 2.5 hr long but used the 600 line  $\text{mm}^{-1}$  grating set at 6200 Å central wavelength.

In 2004, most targeted objects in MS 0451 were selected for deeper follow-up after already being identified as cluster members in our previous year's redshift survey. However, we excluded bright cluster members that had already yielded spectra of sufficient signal-to-noise ratio (S/N) in the 1 hr integrations of 2003. We observed three masks for 4 hr each, with gaps between high-priority targets filled as before with random objects to  $I < 23.0$ . Observations used a 600 line  $\text{mm}^{-1}$  grating set to a central wavelength of 6800 Å.

In 2005 October, objects in both clusters were observed with the same spectral setup and integration times as in 2004, with six masks observed per cluster. However, in 2005 our goal was to follow up on sources detected in both *GALEX* imaging and *Spitzer Space Telescope* MIPS imaging (Geach et al. 2006), and so we filled masks with these sources preferentially. While targets in these latest observations were not selected randomly to a fixed magnitude limit, the total spectroscopic sample is still representative of the cluster as a whole, with the bulk of cluster members identified prior to 2005.

TABLE 2  
MS 0451–03 REDSHIFT CATALOG

$\alpha$ (deg)	$\delta$ (deg)	$z$	Source
73.321434	-3.022260	0.667	1
73.328568	-3.033381	0.370	1
73.325325	-3.024078	0.300	1
73.334717	-3.043395	0.128	1
73.331795	-3.002323	0.539	1
73.344551	-3.028507	0.725	1
73.346550	-3.024269	0.371	1
73.339874	-3.009066	1.160	1
73.337769	-3.004604	0.388	1
73.343781	-3.007794	0.995	1

NOTES.— Table 2 is published in its entirety in the electronic edition of the *Astrophysical Journal*. A portion is shown here for guidance regarding its form and content.

REFERENCES.— (1) Keck/DEIMOS; (2) Ellingson et al. 1998.

DEIMOS data were reduced using the DEEP2 DEIMOS data reduction pipeline (Davis et al. 2003), which produced sky-subtracted, wavelength-calibrated one- and two-dimensional spectra. Redshifts for all galaxies were determined from the one-dimensional spectra and verified by eye. We further correct spectra for the instrumental response curves before measuring line strengths, but we do not perform flux calibration.

In total, we have obtained spectra of over 300 member galaxies per cluster, to  $M_V = -18.0$ , boosting the total known cluster members to 504 in Cl 0024 and 319 in MS 0451. The spectroscopic sample is  $> 65\%$  complete for objects with  $F814W < 21.1$  in Cl 0024 ( $M_V = -19.6$  at the cluster redshift). In MS 0451, completeness to the same absolute magnitude limit is lower,  $\sim 30\%$ , because of the deeper observations required (to  $F814W = 22.0$ ). In both clusters, the spectroscopic sample remains representative of the cluster population as a whole to  $M_V = -19.6$ , roughly 1.5 mag below  $M_*$ . However, in the range  $-19.6 < M_V < -18.0$ , we are biased toward detection of emission-line cluster galaxies over absorption-line galaxies, and completeness is lower in MS 0451 than Cl 0024. In the following, we restrict our analysis to cluster members with  $M_V < -19.6$ , except where specified otherwise.

Our full redshift catalog for Cl 0024 was published in Paper III, excluding the small number of additional redshifts obtained in 2005. In Table 2 we publish a sample of the equivalent full catalog for MS 0451, containing redshifts for 1562 objects. The full catalog is available in the online edition of the Journal.

As Cl 0024 and MS 0451 have now been observed in more detail than perhaps any others at these redshifts, we aim to make as much of our data as practical available to other investigators through our Web site. We will therefore publish updated versions of both the Cl 0024 and MS 0451 catalogs to our Web site,<sup>7</sup> including positions matched with photometric measurements, *HST* morphologies, and redshifts.

### 3.3. Spectral Line Measurement and Velocity Dispersion

We measure spectral line indices for several key emission and absorption lines following the Lick system (Worthey et al. 1994). We focus in this paper on indicators of recent or ongoing star formation, including [O II]  $\lambda 3727$  and the Balmer lines H $\delta_A$  and H $\beta$ , which have been described in Paper III. We also measure the  $D_n(4000)$  index, which indicates the strength of the 4000 Å break; we adopt the definition from Balogh et al. (1999).

<sup>7</sup> See <http://www.astro.caltech.edu/~smm/clusters/>.

TABLE 3  
PHOTOMETRIC AND SPECTROSCOPIC MEASUREMENTS FOR ALL CLUSTER GALAXIES

R.A. (deg)	Decl. (deg)	$z$	Morph	F814W (mag)	$M_r$ (mag)	[O II] ( $\text{\AA}$ )	$D_n(4000)$	$H\delta_A$ ( $\text{\AA}$ )
6.443974	17.141319	0.3792	E/S0	21.9	-18.8	$-25.6 \pm 1.0$	$1.10 \pm 0.02$	$1.6 \pm 0.1$
6.462808	17.145109	0.3978	S0	19.1	-21.7	$2.2 \pm 0.0$	$1.79 \pm 0.01$	...
6.477189	17.274000	0.3967	S0	20.0	-20.7	$-1.8 \pm 0.2$	$1.74 \pm 0.02$	$1.2 \pm 0.1$
6.481423	17.247549	0.3969	Sc+d	20.7	-20.1	$-30.8 \pm 1.7$	$1.20 \pm 0.02$	$5.6 \pm 0.1$
6.499555	17.336269	0.3951	S0	19.9	-20.8	$9.9 \pm 4.1$	...	$-3.8 \pm 0.1$
6.508250	17.056641	0.3992	Sa+b	20.5	-20.2	$-2.4 \pm 0.4$	$1.36 \pm 0.02$	$1.8 \pm 0.2$
6.510695	17.325680	0.3931	S0	19.2	-21.5	$-13.6 \pm 0.5$	$1.77 \pm 0.01$	$-1.8 \pm 0.1$
6.511346	17.324520	0.3913	S0	19.7	-21.0	$-9.4 \pm 0.8$	$1.34 \pm 0.02$	$4.6 \pm 0.1$
6.514315	17.317190	0.3946	E	18.8	-21.9	$1.2 \pm 0.4$	$1.77 \pm 0.02$	...
6.517361	17.105089	0.4059	Sa+b	18.8	-21.9	$1.8 \pm 0.5$	$1.80 \pm 0.02$	$-2.1 \pm 0.1$

NOTES.—Table 3 is published in its entirety in the electronic edition of the *Astrophysical Journal*. A portion is shown here for guidance regarding its form and content.

In order to make maximal use of our spectra for the investigation of stellar populations and SFRs in cluster transition galaxies, we took great care to measure the equivalent widths (EWs) of key spectral lines in an optimal way. We developed a code in IDL that measures EWs via an inverse variance-weighted integration of the flux across the line. The inverse variance ( $1/\sigma^2$ ) for each pixel in a spectrum is automatically generated as output from the DEIMOS reduction pipeline. Weighting by inverse variance minimizes the effects of poorly subtracted sky lines or other low-S/N regions of the spectrum in the calculation of EWs and allows for accurate uncertainty estimates on the indices. The code also robustly measures *lower limits* on emission-line EWs in spectra where emission lines are bright but the underlying stellar continuum is undetected. As in earlier papers, we adopt the convention that emission lines have negative equivalent widths and absorption lines have positive equivalent widths. Hereafter we refer to the equivalent widths in the [O II] line as simply “[O II],” and we refer to  $H\delta$  equivalent widths by the index name, “ $H\delta_A$ .”

In total, we measure EWs for samples of 116 and 124 spiral galaxies in MS 0451 and Cl 0024, respectively, as well as samples of 130 and 109 E+S0s in MS 0451 and Cl 0024, respectively. Photometric characteristics and key spectral line measurements for each of these galaxies are listed in Table 3.

While our spectroscopic sample of cluster members contains no broad-lined AGNs, narrow-lined AGNs are harder to identify due to the lack of  $H\alpha$  in most spectra, complicating identification based on spectral line ratios. In § 4 we therefore must consider the possibility of AGN contamination through other means.

In determining the FP of early-type galaxies (§ 6), we require measurement of the line-of-sight velocity dispersion from the spectra of E+S0 cluster members. Despite a variety of spectral setups, as detailed above, all of our DEIMOS observations yield spectra with a velocity resolution of  $\sim 30\text{--}50 \text{ km s}^{-1}$ . As described in Paper III for Cl 0024, we measure velocity dispersions for MS 0451 early types using the Gauss-Hermite pixel-fitting code of van der Marel (1994) limiting our sample to those observed galaxies with spectral S/N  $> 7 \text{ \AA}^{-1}$ , with a median S/N =  $13 \text{ \AA}^{-1}$ . Extensive testing of this code discussed in Paper III and Treu et al. (2005) implies errors of  $< 10\%$  in the derived velocity dispersions for galaxies above this S/N cutoff. In total, 60 E+S0s in MS 0451 and 71 in Cl 0024 have high-S/N spectra suitable for measurement of the velocity dispersion.

#### 4. PASSIVE SPIRALS

The discovery of passive spirals in clusters at intermediate redshift (Couch et al. 1998; Dressler et al. 1999; Poggianti et al.

1999) has led to their recognition as promising candidates for the role of “transition object” during the theorized conversion of cluster spirals into S0s between  $z \sim 0.5$  and today. Such a conversion, although controversial (e.g., Burstein et al. 2005), has been expected because of the striking contrast between the large number of spirals observed in clusters at  $z \sim 0.5$  and the correspondingly large population of S0s found in clusters locally. In our initial analysis of these passive spirals in Cl 0024 (Moran et al. 2006), we found evidence in their stellar populations for a slow decline in star formation, confirming that passive spirals, at least in Cl 0024, exhibit the prerequisite cessation of star formation needed for any transformation into S0s. Perhaps more importantly, we found that the *abundance* of passive spirals in Cl 0024 is quite high, over 25% of the total spiral population, enough, perhaps, to account for the *entire* buildup of S0s in clusters (but see Kodama & Smail 2001).

However, several questions remain about the nature of passive spirals and their purported S0 end states. Among them are the following: Apart from their lack of emission lines, how do the passive spirals as a class differ from the star-forming spirals, and are their properties uniform between clusters? If they are truly destined to transform into S0s, can we identify directly these new S0s, perhaps just after their new morphologies become firmly in place? Finally, in what environments do the passive spirals reside, and with what implications for the physical mechanisms driving their creation? In this section we attempt to answer the first of these questions, specifying more fully the properties and recent star formation histories of the passive spirals. In §§ 5 and 6 we then consider the next two questions, in our attempt to piece together the full evolutionary history of Cl 0024 and MS 0451 galaxies.

We define as “passive” any spiral with an [O II] equivalent width  $[\text{O II}] > -5 \text{ \AA}$ . Although this definition necessarily allows some contamination from star-forming galaxies that are either moderately dusty or forming stars at a low rate, we demonstrate below via co-added spectra that all emission lines are weak or absent in the passive spirals. We note that we would classify as “passive” many of the spiral galaxies in local clusters that are observed to be  $H\text{ I}$  deficient but retain a low level of star formation (Gavazzi et al. 2006). By examining multicolor (NUV and F814W) imaging of the cluster by eye, we remove from the sample all galaxies where the UV flux is likely to be significantly contaminated by neighboring objects or image artifacts.

We also restrict our passive spiral sample to those objects with  $H\delta_A < 5.0 \text{ \AA}$ ; we assign otherwise passive spirals with  $H\delta_A$  stronger than this to the “poststarburst” category. We note that this  $H\delta$

TABLE 4  
PASSIVE SPIRALS AND UV EMISSION

NAME	FRACTION OF UV-DETECTED SPIRALS (%)		E+S0s (%)	$N_{\text{passive}}/N_{\text{spirals}}$ (%)
	Active Spirals	Passive Spirals		
Cl 0024 .....	$86 \pm 6$	$65 \pm 14$	$25 \pm 7$	$28 \pm 7$
MS 0451 .....	$88 \pm 5$	$37 \pm 15$	$8 \pm 3$	$26 \pm 6$

NOTE.—Above calculations are restricted to  $M_V < -19.6$ , with passive and active spirals defined as described in the text.

limit differs from the definition adopted by some other authors (e.g., Poggianti et al. 1999), who label all passive galaxies with  $H\delta > 3 \text{ \AA}$  as poststarburst. However, the difference is primarily due to different measurement methods for  $H\delta$ : we find that a large number of star-forming and passive spirals exhibit  $3 \text{ \AA} < H\delta_A < 5 \text{ \AA}$  in our sample, which is within the range where Kauffmann et al. (2003) report that star formation histories are consistent with continuous star formation. Therefore, spiral galaxies in our sample with  $[O \text{ II}] > -5 \text{ \AA}$  and  $H\delta_A$  between 3 and 5  $\text{\AA}$  are perhaps more properly called “post–star-forming,” as there is no need to invoke a starburst to explain their  $H\delta_A$  values. We therefore group them with the remainder of the passive spirals.

After culling contaminated objects and dividing our sample according to their  $[O \text{ II}]$  and  $H\delta_A$  strengths, we find that  $87\% \pm 5\%$  of MS 0451 spirals with  $[O \text{ II}]$  emission (brighter than  $M_V = -19.6$ ) are detected in our *GALEX* imaging, similar to the detection rate in Cl 0024. Conversely, only  $37\% \pm 15\%$  of spectroscopically passive spirals are similarly detected (dropping to  $32\% \pm 13\%$  if we were to include the poststarburst spirals), significantly less than the UV-detected fraction in Cl 0024 (see Table 4). As the rest-frame luminosity limits for detection of FUV are virtually the same between the two *GALEX* exposures ( $M_{\text{FUV}} < -17.6$  in MS 0451 and  $M_{\text{FUV}} < -17.9$  in Cl 0024), this represents an important difference in UV luminosity between the two clusters’ passive spiral populations.

In Figure 4 we display the distributions of rest-frame FUV –  $V$  colors for star-forming spirals, passive spirals, and early types in each cluster. It is clear that, despite the overall lower fraction of UV-detected passive spirals in MS 0451, those that are detected exhibit the same intermediate colors as in Cl 0024. To further investigate the colors of passive spirals, and to include those that were not UV detected, we also utilize our ground-based  $R$ - and  $I$ -band imaging to measure rest-frame  $B - V$ , for passive and normal spirals. We observe a trend similar to that seen in the UV–optical colors: the median passive spiral is  $\sim 0.1$  mag redder than the median star-forming spiral in Cl 0024 and 0.2 mag redder in MS 0451. K-S tests indicate that passive spirals have a color distribution significantly different from that of normal spirals, in both clusters.

In fact, we can verify visually that passive spirals appear different from normal star-forming spirals. In Figure 5 we display color postage stamp images of nine spirals in Cl 0024, derived from deep multicolor ACS imaging of the center of Cl 0024, which we retrieved from the *HST* archive (GTO Proposal 10325; PI Ford). In the top row, we display three normal star-forming cluster spirals. The next two rows show cluster passive spirals, which appear to fall into two basic types. Shown in the middle row, some passive spirals appear to retain blue disks, but at surface brightnesses lower than that of star-forming spirals. While some star formation may be occurring in these galaxies, we note that our spectroscopic slits are large enough that we do not believe we are simply “missing” regions of star formation in our observations.

In the bottom row, we see three examples of passive spirals with distinctly red disks, yet with spiral arms and dust lanes still present. These appear similar to the  $z = 0$  “anemic spirals” first identified by van den Bergh (1976); indeed, inspection of the integrated spectrum of a prototypical anemic spiral, NGC 4569 (Gavazzi et al. 2004), indicates that it would likely satisfy our definition of passive spiral. It seems, then, that passive spirals could genuinely be disk-dominated systems where star formation is on the decline or has halted.

In counterpoint to their lower incidence of UV emission, the overall frequency of passive spirals in MS 0451 is quite similar to that found in Cl 0024 (Table 4). In both clusters, more than one-quarter of all spirals are passive, important confirmation that passive spirals are a significant component of both clusters despite the large difference between the clusters’ global properties.

Yet their presence in two quite distinct clusters leads us to question whether the passive spirals are a cluster-related phenomenon at all, or if they could instead represent some fraction

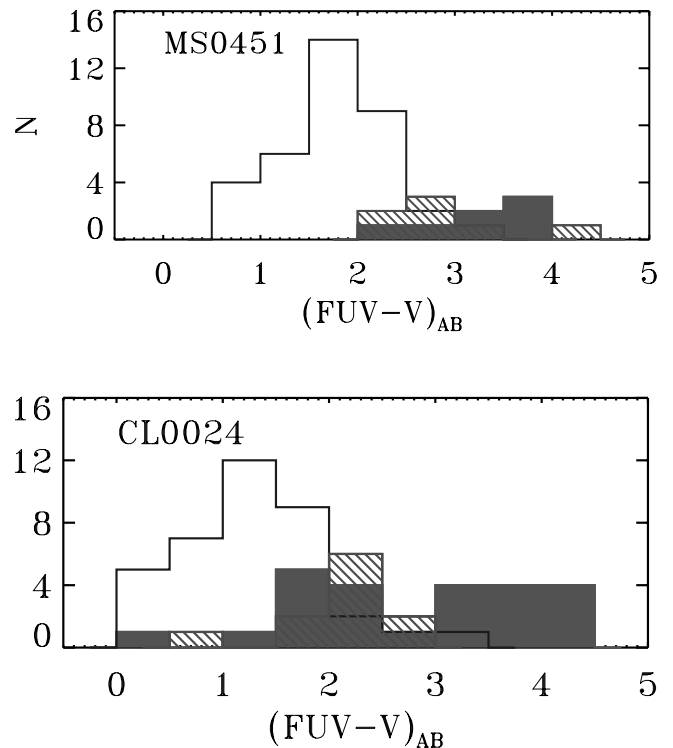


FIG. 4.—Distributions of FUV –  $V$  colors in MS 0451 (top) and Cl 0024 (bottom). Open histograms indicate the colors of normal star-forming spirals. Hatched histograms display the colors for those passive spirals that are detected in the UV, and filled histograms likewise indicate the colors of E+S0s that have been detected in the UV. No correction for dust extinction is applied. UV-detected passive spirals in both clusters have intermediate colors between those of star-forming spirals and those few early types detected in the UV. [See the electronic edition of the *Journal* for a color version of this figure.]

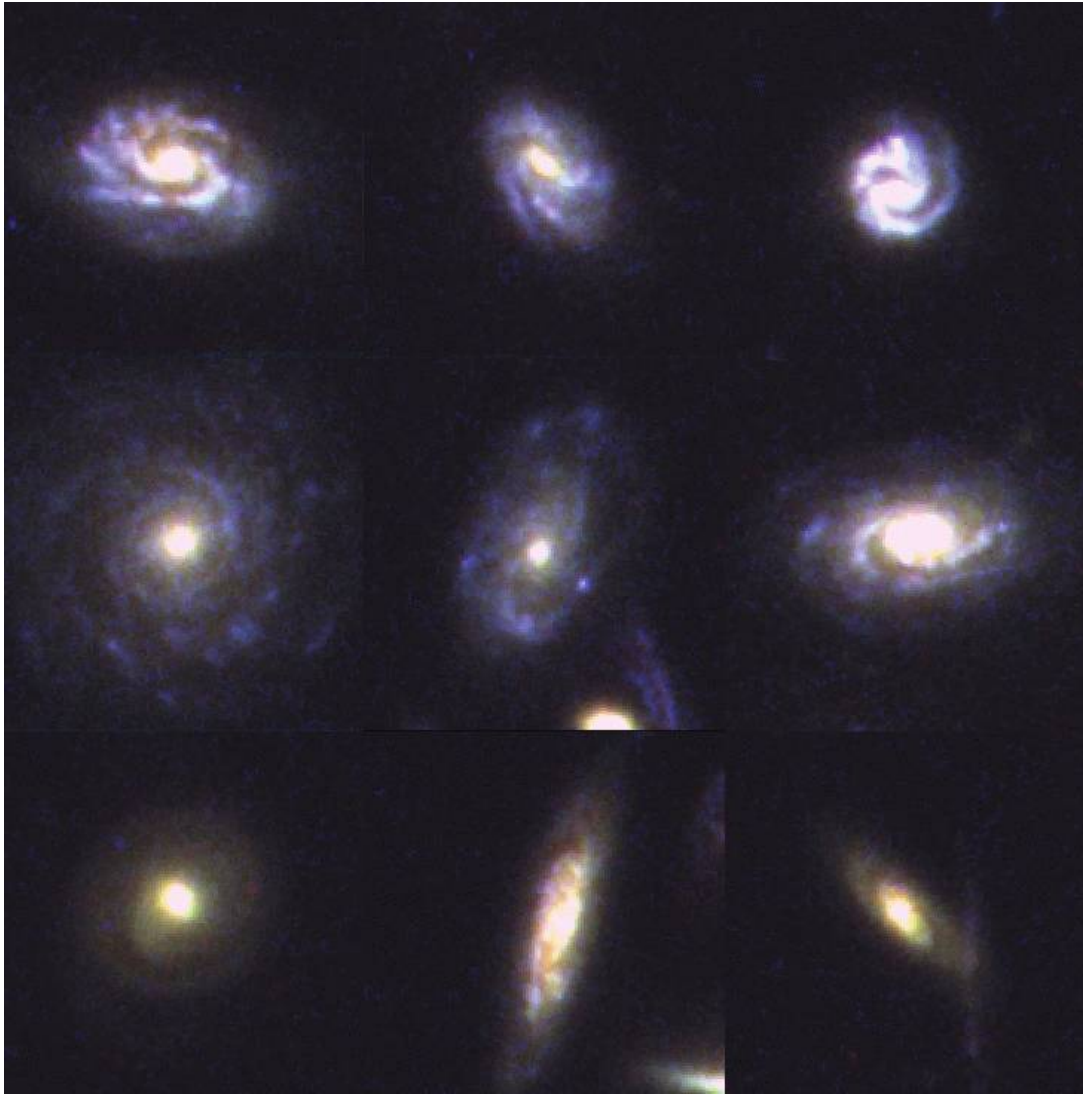


FIG. 5.—Montage of active and passive spirals from deep multicolor ACS imaging of the core of Cl 0024. The top row displays three typical spirals whose spectra exhibit emission lines. The next two rows are composed of passive spirals, which qualitatively exhibit two forms: those with blue disks, but with possibly lower surface brightness than star-forming spirals (*middle row*), and those with distinctly red disks (*bottom row*). All galaxy images are  $4'' \times 4''$  and were extracted from the same multicolor image with identical image scaling and color balance, with F850LP in red, F775W in green, and F555W in blue.

of all spirals that have internally exhausted their star formation. If they are indeed generated in the cluster environment, then we would not expect to find passive spirals in the field at these same intermediate redshifts. We have therefore examined a sample of 105 field spirals in the redshift range  $0.3 < z < 0.65$ , identified in the course of our spectroscopic campaign. Out of 62 galaxies where [O II] falls within our wavelength coverage, we measure a passive spiral fraction of only  $6\% \pm 3\%$ . This low incidence in the field confirms that the generation of passive spirals is a cluster-related phenomenon at these redshifts (Poggianti et al. 1999). The  $6\% \pm 3\%$  of passive spirals found in the field may indicate that some passive spirals can be formed in groups.

Despite their overall similar abundance in both clusters, the weaker UV emission in MS 0451 passive spirals presents a puzzle that leads us to again consider the different assembly states and ICM properties of the two clusters. To more precisely quantify the nature of the passive spirals in each cluster, we introduce as a key diagnostic plot the  $FUV - V$  versus  $D_n(4000)$  diagram.  $D_n(4000)$  is sensitive to stellar populations with ages of  $\sim 2$  Gyr, with a dependence on metallicity that only becomes apparent for

old stellar populations (Poggianti & Barbaro 1997), while the  $FUV - V$  color is sensitive to star formation on a much shorter timescale ( $10^7 - 10^8$  yr). As seen below, comparing  $D_n(4000)$  to  $FUV - V$  color provides a valuable tool to discriminate between different star formation histories for passive and star-forming spirals.

In Figure 6 we plot  $D_n(4000)$  versus rest-frame  $FUV - V$  color for MS 0451 (*top panel*) and Cl 0024 (*bottom panel*). It is clear from the diagram that most star-forming spirals in both clusters exhibit blue  $FUV - V$  color (median of  $1.6 \pm 0.1$ ) combined with weak  $D_n(4000)$  strength (median  $1.22 \pm 0.02$ ). Such values indicate young stellar populations and are expected for galaxies with ongoing star formation.

Turning to examine the locations of passive spirals, we note that passive spirals in MS 0451 largely occupy a different region of the plot than Cl 0024 passive spirals. Cl 0024 passive spirals with UV detections (the majority) cluster quite tightly on the plot at moderate  $FUV - V$  colors (median  $2.5 \pm 0.1$ ) and moderately strong  $D_n(4000)$  (median  $1.47 \pm 0.02$ ). In contrast, as we have already noted, many of the MS 0451 passive spirals have only

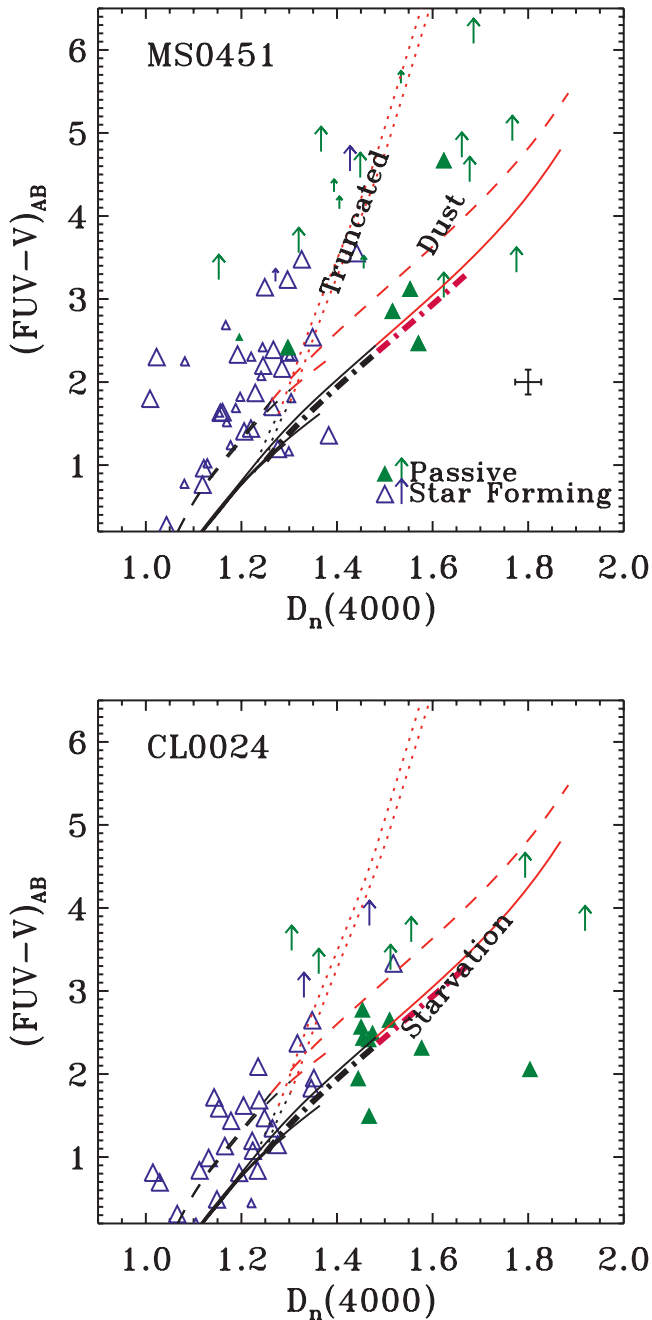


FIG. 6.—FUV  $- V$  colors vs.  $D_n(4000)$  strength for spirals in MS 0451 (*top*) and Cl 0024 (*bottom*). Star-forming and passive spirals are indicated by open blue triangles and filled green triangles, respectively. Arrows denote  $3\sigma$  lower limits for FUV  $- V$  colors for those galaxies not detected in the UV, colored blue for star-forming spirals and green for passive spirals. Small triangles or lower limit arrows indicate spirals with  $H\delta_A > 5 \text{ \AA}$ , similarly color-coded. We plot only galaxies with especially small uncertainty in  $D_n(4000)$ ,  $< 0.07$ . Solid, dashed, dotted, and dot-dashed lines, respectively, indicate model tracks for exponentially declining, dust-enshrouded, truncated, or starved star formation, as described in the text. Tracks are colored red for regimes where  $[O \text{ II}] > -5 \text{ \AA}$ . Most UV-detected passive spirals are consistent with a starvation model, while most undetected passive spirals are better fitted by a rapid truncation of star formation.

upper limits on their FUV emission, some at quite red FUV  $- V$  colors. Across both clusters, these UV-undetected objects seem also to exhibit a wider spread in  $D_n(4000)$  than the UV-detected passive spirals (rms of  $0.23 \pm 0.06$  vs.  $0.08 \pm 0.02$ ). The dominance of UV-detected passive spirals in Cl 0024, compared to

the UV-undetected type that are predominant in MS 0451, begs the question of whether passive spirals are created in different ways in each of the two clusters. As we show below, the two types of passive spirals, UV detected and undetected, may have fundamentally different star formation histories.

To help decipher the star formation histories of passive spirals in Cl 0024 and MS 0451, we overlay in Figure 6 evolutionary tracks from the population synthesis code of Bruzual & Charlot (2003), adopting fixed solar metallicity for all models. Using these, we can test several classes of models that could explain the origin of passive spirals. Specifically, can passive spirals be created by simply adding dust to a star-forming spiral? Can they be created by suddenly switching off star formation in a galaxy, which we call “truncation” models? Or, finally, can we create the passive spirals by switching a star-forming spiral into a phase where its SFR declines more rapidly over a timescale of 0.5–2 Gyr (a starvation model)?

In Figure 6, solid lines indicate the track followed in FUV  $- V$  versus  $D_n(4000)$  space by several model stellar populations with exponentially declining SFRs, with characteristic timescales  $\tau \sim 3\text{--}7$  Gyr. Such models have been found to reproduce the optical spectra of Sa–Sc type star-forming galaxies (Poggianti & Barbaro 1996). Dashed lines add dust extinction of  $A_V = 0.6$  to these same models, corresponding to the mean difference in FUV  $- V$  between the (UV detected) passive and active spirals. Active spirals largely occupy the region in between tracks with zero and moderate extinction. Tracks are in red for regimes where  $[O \text{ II}] > -5 \text{ \AA}$ , estimated from the models in the same way as in Moran et al. (2006).

Only models with a relatively fast exponential decline in SFR ( $\tau \leq 1$  Gyr; *upper solid and dashed lines in Fig. 6*) can match the peculiar combination of intermediate FUV  $- V$  and strong  $D_n(4000)$  exhibited by the bulk of the UV-detected passive spirals. Any star-forming spirals that transition into this sort of rapid decay of star formation, eventually entering a spectroscopically passive phase, will reproduce the positions of the UV-detected passive spirals in the diagram (*thick dot-dashed “Starvation” line in Fig. 6*).

Conversely, passive spirals with lower limits on their color, which dominate the population in MS 0451, seem to be most consistent with models where star formation is rapidly truncated at an age  $< 7$  Gyr, indicated by the dotted lines in Figure 6. Stacking together the UV images for undetected passive spirals, we still detect no significant UV emission. Although confusion noise becomes significant in the stacked image, the nondetection implies that the median FUV  $- V$  is at least  $\sim 1$  mag fainter than the upper limits indicated in Figure 6.

The positions of these UV-undetected spirals on the plot could also be explained by strong levels of dust obscuration. However,  $24 \mu\text{m}$  imaging of both clusters with MIPS on the *Spitzer Space Telescope* indicates that there is a deficit of obscured dusty starbursts in MS 0451, in comparison to Cl 0024 (Geach et al. 2006). If the UV-undetected passive spirals were simply dusty, we would expect to see the *opposite* trend in the MIPS observations, since there are so many of these objects in MS 0451. We therefore believe that the rapid truncation of star formation is the most likely explanation for the UV-undetected passive spirals.

The population of spirals in MS 0451 includes a number of poststarburst galaxies that also seem to be consistent with rapidly truncated star formation; in fact, rapid truncation of a starburst is thought to be the primary way that these galaxies achieve such high  $H\delta_A$  values (Poggianti et al. 1999). Indeed, the poststarburst spirals may be closely related to the UV-undetected passive spirals in MS 0451. Several apparently star-forming galaxies also reside

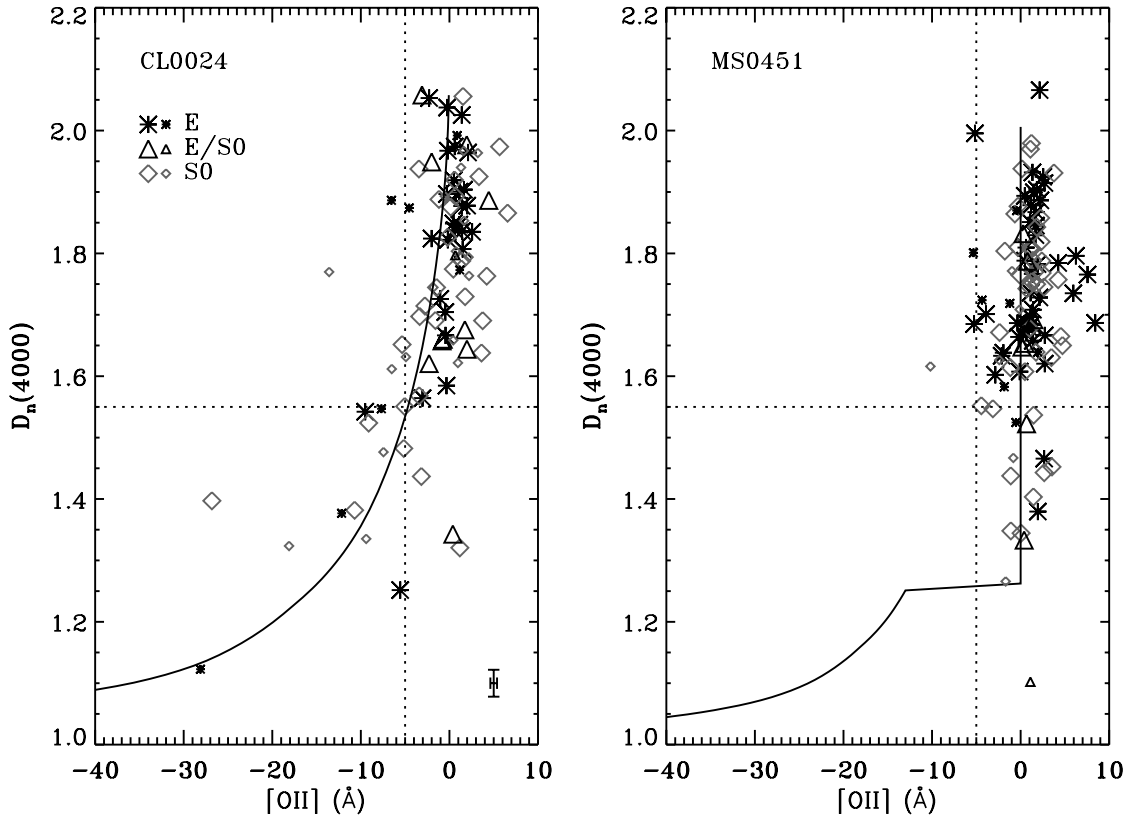


FIG. 7.— $D_n(4000)$  Balmer break strengths vs.  $[O II]$  equivalent widths for cluster early types in Cl 0024 (*left*) and MS 0451 (*right*). Symbol shapes and shades denote galaxy morphologies as indicated in the figure, with median error bar indicated at lower right (*left*). Small symbols indicate galaxies that are located outside the cluster virial radius, and large symbols mark galaxies within  $R_V$ . Vertical and horizontal dotted lines, respectively, indicate  $[O II] = -5 \text{ \AA}$  and  $D_n(4000) = 1.55$  (See text). The solid line in the left panel is the best-fitting model track, a starvation ( $\tau = 1 \text{ Gyr}$ ) model with dust, while in the right panel the best fit is to a truncation model (at age 5 Gyr). The best-fit model tracks for each cluster are similar to those seen in Fig. 6. [See the electronic edition of the Journal for a color version of this figure.]

along the truncated track. Together, these could represent a continuum of galaxies in various stages of having their star formation halted. However, the supposedly rapid timescale for the cessation of star formation begs the question of why we would see any star-forming spirals in the region of the plot where models indicate that they should already be passive. Some mix of models, with increased dust obscuration combined with the truncation of star formation, could provide an explanation.

While we have found passive spirals to be abundant in both Cl 0024 and MS 0451, it appears that they are largely formed through different mechanisms in each cluster. The more rapid cessation of star formation required to explain the MS 0451 passive spirals is likely due to some physical mechanism that exerts a stronger force on galaxies in MS 0451 than in Cl 0024. This once again brings to mind the hot, dense ICM of MS 0451, which at least has the potential to apply a much stronger force (ram pressure stripping) on infalling galaxies than in Cl 0024. In the next section we examine the stellar populations of early-type galaxies across the two clusters, in an attempt to identify the expected end products of these rapidly and slowly quenched passive spirals: S0s with signatures of recent star formation on varying timescales.

### 5. THE STAR FORMATION HISTORIES OF E+S0 GALAXIES

While careful analysis of local S0 galaxies has revealed some signs that their stellar populations are younger than those of ellipticals (e.g., Poggianti et al. 2001), such signatures have so far been elusive at intermediate redshift, despite expectations that S0s

with newly halted star formation would be abundant. Now, however, under the hypothesis that passive spirals in MS 0451 and Cl 0024 must be disappearing from our spiral sample as they fade in UV and increase in  $D_n(4000)$ , we turn again to a study of the stellar populations of early-type galaxies.

The different characteristics of passive spirals in Cl 0024 and MS 0451 help to provide a key for uniquely linking the passive spirals to their potential S0 descendants. Because the properties of passive spirals largely differ between the two clusters, so too will any S0s that have just recently changed their morphology.

With this in mind, we wish to examine recent star formation, as well as any ongoing star formation in the cluster E+S0s. In Figure 7 we plot  $D_n(4000)$  strength versus  $[O II]$  equivalent width for all early types in Cl 0024 (*left panel*) and MS 0451 (*right panel*), with symbols coded to indicate their morphologies (as shown in the legend).

Most bright E+S0s in both clusters exhibit the signatures of old stellar populations: weak or absent  $[O II]$  and a strong Balmer break [ $D_n(4000) \gtrsim 1.6$ ]. In Cl 0024, however, we observe a striking tail of galaxies extending from the locus of old E+S0s toward weaker  $D_n(4000)$ , coupled with significant  $[O II]$  emission. MS 0451 exhibits a similar tail of early-type galaxies toward weak  $D_n(4000)$  strength, but *without* any associated  $[O II]$  emission.

If we apply a cut at  $D_n(4000) = 1.55$ , indicated by the horizontal dotted lines in the figure, we find that 10%–15% of the total E+S0 population in each cluster has  $D_n(4000)$  below 1.55. While somewhat arbitrary, the chosen  $D_n(4000)$  dividing line lies well below the expected value for an early-type galaxy that has been passively evolving since formation at  $z \geq 1$ . In fact, in

the case of a prototypical elliptical whose stars were created in a short burst,  $D_n(4000)$  should fade from 1.25 to 1.7 in less than  $\sim 2$  Gyr, according to Bruzual & Charlot (2003) models, which is less than the time from  $z = 1$  to  $\sim 0.5$ .

There are essentially two possible explanations for finding E+S0 galaxies with such low  $D_n(4000)$ : either they have undergone recent star formation, or they harbor an AGN that contributes to the spectrum. If they have formed stars recently or are continuing to form stars, then they must have either formed a significant population of stars at  $z < 1$  while already displaying early-type morphology or else transformed morphology from a star-forming spiral to an early type (either singularly or through a merger). Under each of these scenarios, there must be some way to account for the presence of emission lines in the C1 0024 objects but a lack thereof in MS 0451.

A third possibility, that we have simply misclassified some spiral galaxies as S0s, is easy to discount based on this last requirement. If the low- $D_n(4000)$  S0s are truly just spirals, then we would not expect in MS 0451 to *exclusively* miscast as S0 just those spirals with no [O II] emission, while at the same time misclassifying spirals with a range of [O II] in C1 0024. On the other hand, if we are biased toward mixing up the morphological classifications of passive spirals and S0s, this only strengthens the notion that one type may be transforming into the other.

To better assess the star formation histories of these peculiar objects, we overplot in Figure 7 two characteristic model tracks equivalent to those plotted for the passive spirals in Figure 6. In C1 0024, we plot a starvation-like track ( $\tau = 1$  Gyr with internal  $A_V = 0.6$ ), while in MS 0451, we plot the track of a galaxy with star formation truncated rapidly at an age of 5 Gyr. In each case, the model track reproduces the positions of the galaxies very well. We note that most physically plausible truncated-spiral tracks are inconsistent with the distribution of points in C1 0024, as no such models reach  $D_n(4000) \gtrsim 1.4$  before truncation, yet we still see galaxies with [O II] emission in this range. Remarkably, then, a single starvation track reproduces the positions of both the low- $D_n(4000)$  early types and most passive spirals (Fig. 6) in C1 0024, while a truncated star formation track similarly matches the star formation histories of both classes in MS 0451. These similarities in star formation history suggest an evolutionary link between the passive spirals and the low- $D_n(4000)$  early types in each cluster.

We can further evaluate the likelihood of a connection between the passive spirals and the low- $D_n(4000)$  early types through a consideration, for each cluster, of the co-added spectra of both classes. In Figure 8 we plot in the top panel the co-added spectra of all E+S0s in the clusters with  $D_n(4000) < 1.55$  and in the bottom panel the co-added spectra of passive spirals in each cluster. In each case, we only include galaxies with overall spectral  $S/N > 5.0 \text{ \AA}^{-1}$  in the summation. The locations of several key spectral lines are marked.

Considering the co-added early types first, we can immediately cast doubt on the idea that AGNs are responsible for the low  $D_n(4000)$ . While a substantial contribution from a flat AGN continuum can serve to weaken the Balmer break in a galaxy, the same effect should also dilute the observed depth of stellar absorption lines, such as  $H\delta_A$ . Yet it is clear from the co-added spectra that the low- $D_n(4000)$  early types in both clusters exhibit moderately strong  $H\delta_A$ :  $2.2 \pm 0.2$  and  $1.2 \pm 0.2 \text{ \AA}$  for MS 0451 and C1 0024, respectively. As both values are much higher than the median  $H\delta_A = -1.0 \pm 0.2$  of cluster ellipticals, their Balmer strengths are consistent with the interpretation that they contain young stars and *inconsistent* with a significant AGN (dust obscured or otherwise) contributing to the galaxy's spectrum.

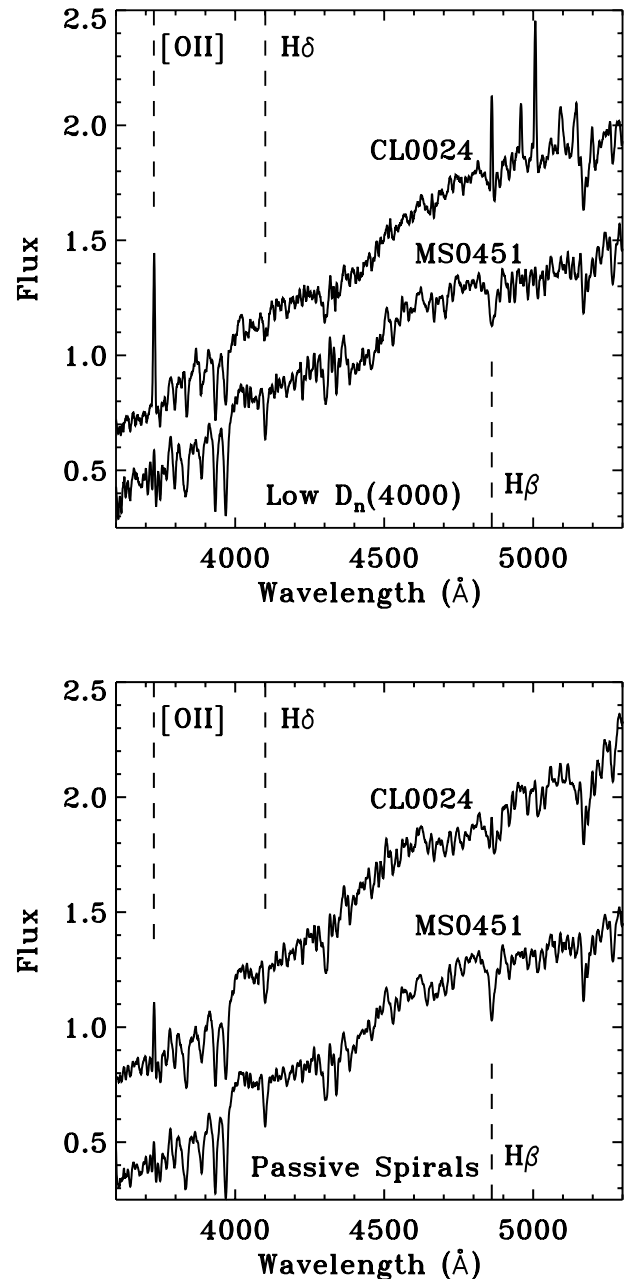


FIG. 8.—*Top*: Normalized, co-added spectra of E+S0s in C1 0024 and MS 0451 with  $D_n(4000) < 1.55$ , including only spectra with  $S/N > 5 \text{ \AA}^{-1}$ . The C1 0024 spectrum is shifted upward in flux (arbitrary units) for display purposes. The locations of several key spectral lines are marked. *Bottom*: Normalized, co-added spectra of passive spirals in C1 0024 and MS 0451, also restricted to spectra with  $S/N > 5.0 \text{ \AA}^{-1}$ . In each cluster, the [O II],  $H\delta_A$ , and  $H\beta$  strengths of passive spirals closely resemble those of the low- $D_n(4000)$  early types in the same cluster.

Although the spectra make clear that these “young S0s” (as we call them) truly contain a population of young stars, is it possible that these galaxies have recently undergone a “rejuvenation” of star formation through some interaction? Serious doubt is cast on this hypothesis by the lack of MS 0451 E+S0s currently containing emission lines in their spectra. After a moderate starburst on top of an established stellar population, Bruzual & Charlot (2003) models predict a return to a passive spectrum with strong  $D_n(4000)$  in as little as 100 Myr after the burst. To have so many S0s experience a rejuvenation episode so recently, yet observe none of them currently in a starburst phase, is implausible.

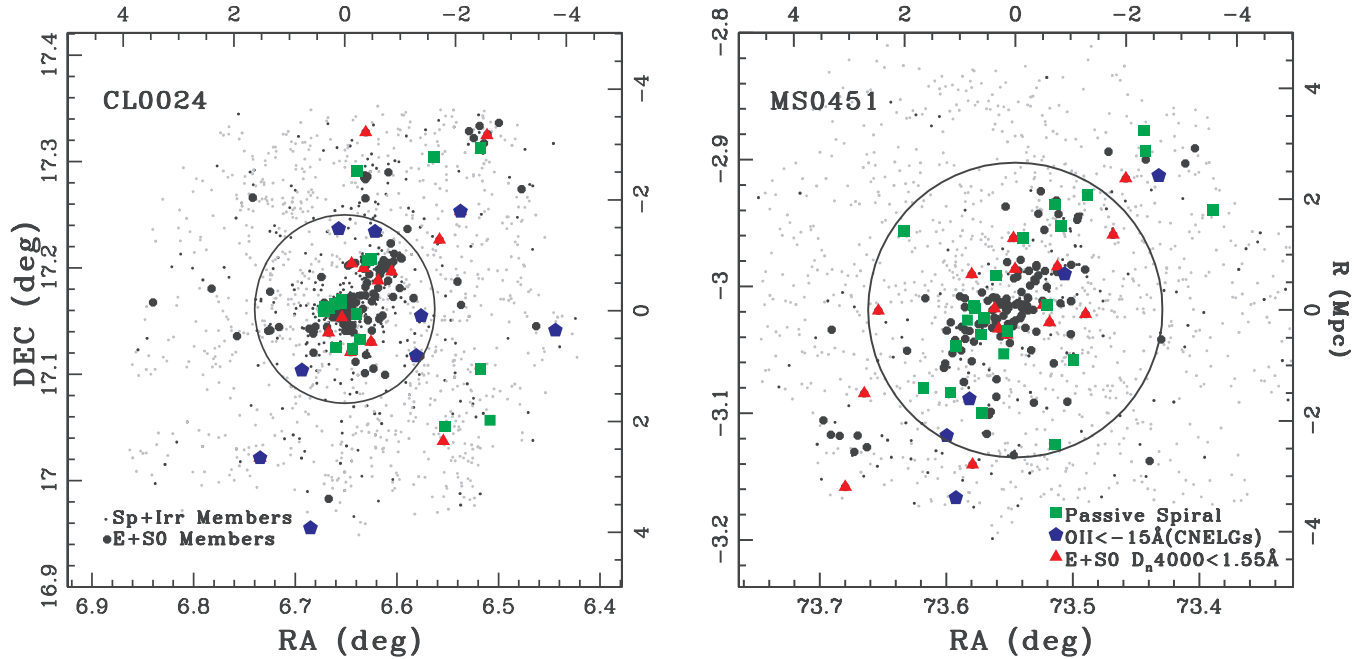


FIG. 9.— Distribution of galaxies in the field of Cl 0024 (*left*) and MS 0451 (*right*). Galaxies showing spectroscopic signs of recent evolution are marked. Spectroscopically confirmed cluster members are marked with large (E+S0s) and small (spirals) black dots. Objects with spectroscopically determined redshifts outside the cluster are marked as gray dots. Blue pentagons are CNELGs ( $[\text{O II}] < -15 \text{ \AA}$ , and to  $M_V < -18.0$ ). Filled green squares are passive spirals. Filled red triangles mark early types with  $D_n(4000) < 1.55$ . Top and right axes show projected radius from the cluster center, in Mpc. The large circle indicates the virial radius in each cluster. Passive spirals and young S0s are found even in the outskirts of both clusters, perhaps residing in groups.

We are left, then, with the possibility that these young S0s truly represent the end states of the passive spirals. The contrast between young S0s in Cl 0024, whose  $[\text{O II}]$  strengths are consistent with a gradual decline in star formation, and those in MS 0451, where the lack of  $[\text{O II}]$  indicates recent truncation, evokes the similar dichotomy between passive spirals with a slow truncation of star formation (mostly in Cl 0024) and those exhibiting a more rapid truncation (mostly in MS 0451). Comparing the co-added spectra of the two classes in more detail, we find further evidence to support an evolutionary link between passive spirals and young S0s.

First, the passive spiral spectrum for Cl 0024 exhibits a weak  $[\text{O II}]$  emission line of  $-3.1 \pm 0.5 \text{ \AA}$ , despite the population having been selected for their low  $[\text{O II}]$ . The presence of some  $[\text{O II}]$  emission in both the passive spirals and the young S0s ( $[\text{O II}] = -10.1 \pm 0.5 \text{ \AA}$ ) is consistent with the slow decay in star formation thought to be acting. It may be that, in some cases, the transformation to S0 morphology occurs *before* the final cessation of star formation. MS 0451 passive spirals, in contrast, have an  $[\text{O II}]$  equivalent width consistent with zero, as do their S0 counterparts. Again, this is consistent with the rapid truncation of star formation in MS 0451 passive spirals, followed by an almost simultaneous transformation into S0 morphology. The morphological transformation cannot be significantly delayed after the halt in star formation because the S0s' low  $D_n(4000)$  and strong  $H\delta_A$  strictly limit the time since last star formation to  $< 100$  Myr, according to the model tracks in Figures 6 and 7.

Secondly, the  $H\delta_A$  values of passive spirals in each cluster are similar to those of their counterpart young S0s. In Cl 0024, passive spirals exhibit weaker  $H\delta_A$  than normal star-forming spirals:  $H\delta_A = 1.8 \pm 0.2 \text{ \AA}$  in the co-added spectrum compared to a median  $H\delta_A = 3.9 \pm 0.2 \text{ \AA}$  for star-forming spirals (see also Moran et al. 2006). The co-added spectrum of young S0s exhibits a similarly moderate  $H\delta_A = 1.2 \pm 0.2 \text{ \AA}$ , between the typical values for spirals and for ellipticals. In MS 0451, passive spirals

( $H\delta_A = 3.0 \pm 0.2 \text{ \AA}$ ) and young S0s ( $H\delta_A = 2.2 \pm 0.2 \text{ \AA}$ ) exhibit  $H\delta_A$  strengths that also mirror each other closely. Yet they exhibit overall higher strengths than in Cl 0024, another indication that the halt in star formation was quite recent for galaxies in MS 0451.

The close similarities between passive spirals and young S0s *within* each cluster, coupled with the clear differences in populations *between* the two clusters, strongly argue in favor of a model where passive spirals and young S0s represent an evolutionary sequence. At the same time, we have not yet fully explored possible explanations for why this evolutionary sequence behaves differently in the two clusters. In the next section we begin consideration of this issue by examining the local environments in which passive spirals and young S0s are found.

## 6. THE ENVIRONMENTS OF PASSIVE SPIRALS AND YOUNG S0s

So far, we have treated the populations of passive spirals and young S0s largely as a uniform population within each cluster. The reality, however, is more complex. While the passive spirals in MS 0451 were largely found to have different star formation histories than Cl 0024 passive spirals, the segregation is imprecise: MS 0451 contains a proportion of UV-detected spirals ( $\sim \frac{1}{3}$ ) consistent with a slow decline in star formation, while Cl 0024 conversely contains a similar fraction of passive spirals whose star formation may have been truncated more rapidly. To help disentangle this puzzle, we focus now more closely on the local environments in which the passive spirals and their remnant S0s are found.

We start by examining the spatial distribution of transition galaxies across both clusters. In Figure 9 we plot the positions of all passive spirals (*green squares*) and young S0s (*red triangles*). We also plot the populations of compact narrow emission line galaxies (CNELGs) found in each cluster (*blue pentagons*), which are discussed further in § 7.

The first striking feature to note in Figure 9 is that passive spirals and young S0s occur both in the cluster core and at higher radius, even beyond  $R_V$ , with no obvious segregation between the passive spirals and S0s. Secondly, in MS 0451 both passive spirals and young S0s appear to be more spread out across the cluster than in Cl 0024, where more than half are located within 1 Mpc of the cluster center. Both features reveal important clues to the physical processes at work.

Careful inspection of those passive spirals found beyond the cluster cores gives the impression that many have other cluster members nearby. Could passive spirals be preferentially found in infalling groups? Some evidence for passive spirals in groups at these redshifts has already been noted (Jeltema et al. 2007). To evaluate quantitatively this possibility, we calculate the projected local densities of these passive spirals, using the 10 nearest neighbors method, following Paper I and Dressler et al. (1997). Considering only galaxies outside of the cluster cores ( $R > 1$  Mpc in Cl 0024 and  $R > 1.5$  Mpc in MS 0451,  $\sim 50\%$  of  $R_V$ ), we find that passive spirals are found at a median local density of  $\Sigma = 36 \pm 5 \text{ Mpc}^{-2}$  in MS 0451 and  $\Sigma = 51 \pm 15 \text{ Mpc}^{-2}$  in Cl 0024, both somewhat higher than the density of a typical infalling spiral of  $\Sigma = 28 \pm 3 \text{ Mpc}^{-2}$  across both clusters.

Passive spirals, therefore, seem to be forming both within infalling groups and closer to the cluster core, two distinct regions where the dominant physical forces acting on galaxies are likely to be quite different. Remarkably, we find that four out of the five UV-detected passive spirals in MS 0451 reside in groups outside the cluster core. Recalling from Figure 6 that these UV-detected passive spirals closely follow a “starvation-like” gradual cessation of star formation, we conclude that *nearly all* passive spirals within infalling groups are experiencing a cessation of star formation spread over a  $\sim 1$  Gyr timescale.

In contrast, virtually all MS 0451 passive spirals within 1.5 Mpc of the cluster center have undergone a rapid truncation in star formation. In Cl 0024 it appears that rapid truncation of star formation can also occur, but only extremely close to the cluster core: four out of six passive spirals without UV detection are located within 300 kpc of the Cl 0024 center.

While passive spirals are abundant in the region around the MS 0451 center, there is a hole of  $\sim 600$  kpc radius, within which we observe almost no spirals of any type. Unlike in Cl 0024, where spirals are observed even within  $\sim 100$  kpc of the central galaxies, no spirals survive to reach the center of MS 0451. Even accounting for the larger virial radius of MS 0451, this spiral-free zone is significantly larger than that seen in Cl 0024: within  $0.2R_V$  ( $\sim 530$  kpc in MS 0451 and  $\sim 340$  kpc in Cl 0024), only  $4\% \pm 3\%$  of MS 0451 members in our sample are spirals ( $< 2\%$  passive), compared to  $42\% \pm 7\%$  ( $9\% \pm 3\%$  passive) in Cl 0024. As the time required for a galaxy to travel  $\sim 600$  kpc across the core of MS 0451 is only 0.4 Gyr, it appears that spirals in this environment must indeed be converted to early morphology quite rapidly.

Both the central hole in MS 0451 and the central concentration of UV-undetected passive spirals in Cl 0024 can be better understood by considering the local ICM densities of the transition galaxies in each cluster. In Figure 10 we make use of *Chandra* X-ray data for each cluster to plot the expected strength of ram pressure as a function of radius for Cl 0024 and MS 0451. Each track is generated by calculating the gas density  $\rho(R)$  from the best-fit isothermal  $\beta$ -model from Donahue et al. (2003) and Ota et al. (2004) for MS 0451 and Cl 0024, respectively. We then estimate ram pressure  $P = \rho v^2$  by adopting each cluster’s line-of-sight velocity dispersion,  $\sigma$ , as the characteristic velocity of a galaxy in that cluster.

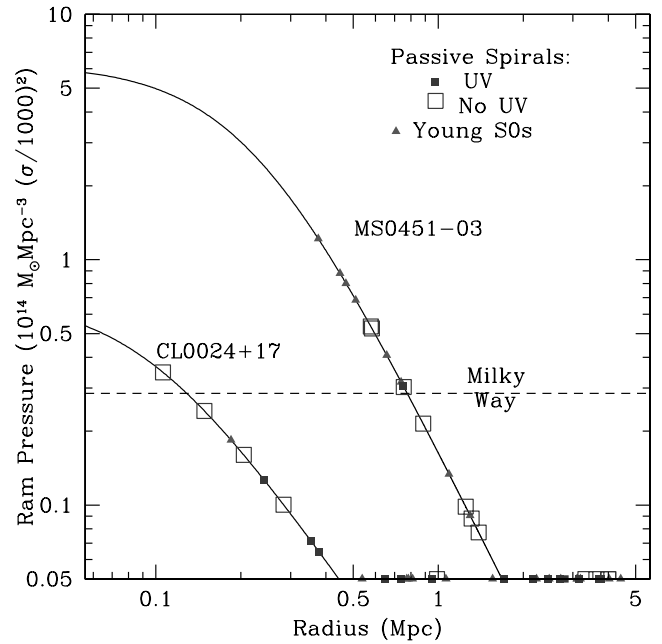


FIG. 10.—Strength of ram pressure as a function of radius, for both Cl 0024 and MS 0451. Solid lines indicate ram pressure  $P(R)$  as described in the text. The dotted line indicates the pressure required to strip a spiral with characteristics of the Milky Way (Paper I; Gunn & Gott 1972). Overplotted on each track are the radial positions of passive spirals (UV detected and undetected) and young S0s in that cluster. Where the ram pressure falls below the lower bound of the plot, we mark the positions of galaxies along the lower edge of the plot. Most UV-undetected passive spirals are found in regimes of high ram pressure, while no passive spirals survive in regimes where ram pressure is more than a few times that required to strip a Milky Way-like spiral. [See the electronic edition of the Journal for a color version of this figure.]

Figure 10 reveals that virtually all UV-undetected passive spirals are found in regimes where the ram pressure is significant ( $> 20\%$  of that required to strip a Milky Way analog), while UV-detected passive spirals are largely confined to regions of lower gas density. While the corresponding radial ranges differ between Cl 0024 and MS 0451, the UV-undetected passive spirals span a nearly identical range of ram pressure strengths in each cluster. This argues strongly in favor of ram pressure stripping as the mechanism responsible for the UV-undetected passive spirals. We note that no spirals survive in environments where the ram pressure is more than a few times that required to strip the Milky Way, and a natural consequence of this limit is that no spirals in MS 0451 survive to reach  $R < 600$  kpc (although, as expected, several young S0s appear at slightly lower radii). In § 7.2 we discuss in more detail the relation between this presumed ram pressure stripping and other mechanisms that may be acting to transform morphology.

## 7. PHYSICAL PROCESSES DRIVING THE TRANSFORMATION

So far, we have shown in §§ 4 and 5 that the large populations of passive spiral galaxies in both Cl 0024 and MS 0451 are transforming into S0s on a variety of timescales. Building on this, in § 6 we have successfully matched the timescales of transformation with specific environments within each cluster. Consequently, we are now able to construct a road map describing the sites and timescales of transformations across both clusters.

To summarize, we find that some passive spirals are generated within infalling groups, experiencing a gradual decline in SFR and eventual transformation to S0 morphology. In the central regions of both clusters, a high proportion of spirals are seen to be

passive. In Cl 0024, star formation within these spirals continues to decay at a relaxed pace, with few signs of rapid interaction with the cluster environment except near the very center where the effects of ram pressure begin to be important. In contrast, passive spirals all across the core of MS 0451 have had their star formation truncated rapidly, with a subsequent rapid transformation into S0 morphology.

In this section we use this road map to consider the constraints that we can place on the physical processes operating in each of these three regimes: groups in the cluster outskirts, the Cl 0024 core, and the MS 0451 core.

### 7.1. The Cluster Outskirts

In the hierarchical assembly of clusters, groups infalling from the cluster outskirts can be thought of as the building blocks. Paper I argued that the existence of the morphology-density relation implies that a galaxy's evolutionary history is tightly linked to its group's history, until the group is absorbed into the cluster. Furthermore, the observation that mass and light trace each other tightly on large to small scales (Paper II) suggests that groups of roughly constant mass-to-light ratio, rather than individual galaxies, coalesce to build up the cluster.

The preprocessing of galaxies within these infalling groups is a crucial feature of evolution within both clusters, as here we are probing galaxies in a key density range at a key point in time: at  $z > 0.5$ , observations indicate that the early-type fraction is growing only in the cores of clusters, while below  $z \sim 0.5$  evolution begins to accelerate in lower density regions (Smith et al. 2005a; Postman et al. 2005). As such, gaining an understanding of the physical processes driving galaxy transformation within the infall regions of clusters at  $z \sim 0.5$  can shed light on the observed evolution in the morphology-density relation.

By virtue of the fact that passive spirals in the cluster outskirts are preferentially found in groups, we do not expect that the clusters' ICM plays a direct role in suppressing star formation. Even in MS 0451, the force of the ICM should not be significant beyond the virial radius (Fig. 1). And while we had previously argued in favor of starvation by the ICM (Moran et al. 2006), which can be effective at large cluster radius, there is little reason to expect it to act on galaxies in groups more effectively than isolated spirals.

However, we cannot rule out the presence of gaseous interactions *within* groups. Indeed, X-ray observations of groups in the local universe reveal that they often harbor an intragroup medium (Mulchaey 2000), and simulations by Bekki et al. (2002) suggest that the starvation mechanism can operate similarly within large groups as it would in the overall cluster (see also Hester 2006; Fujita 2004). Intriguingly, X-ray-bright groups seem to contain a higher early-type fraction than X-ray-undetected groups (Zabludoff & Mulchaey 1998), consistent with the notion that the gas plays a role in shaping galaxy morphology.

The predicted timescale for cessation of star formation under starvation is consistent with our observed decline over 0.5–2 Gyr (Fujita 2004); in simulations by Okamoto & Nagashima (2003) a timescale of 1–2 Gyr for the halt in star formation after gas removal provided a good fit to observations. We emphasize, however, that the  $\sim 1$  Gyr decline in star formation represents only one observable phase of the predicted total timescale for conversion of a spiral to an S0 via starvation ( $\geq 3$  Gyr; Bekki et al. 2002; Boselli et al. 2006). The slow action of starvation would preserve recognizable spiral structure for over 1 Gyr after star formation stops, and we have shown in Moran et al. (2006) that these lifetimes for each phase are consistent with the hypothesis that all such passive spirals will become S0s by  $z = 0$ .

Yet direct observations of the intragroup gas are challenging at these redshifts, especially for small groups (but see Jeltema et al. 2007), and other mechanisms may also be able to reproduce the observed timescale for the cessations of star formation. In addition, some models suggest that modification of SFRs due to starvation only begins to be visible many gigayears after the halo is stripped (Boselli et al. 2006), and so the effectiveness of starvation in groups would depend in some sense on the dynamical age of each group, which is difficult to quantify. Gentle gas stripping or starvation by a diffuse intragroup medium therefore remains an attractive, but difficult to test, possibility.

Alternatively, the increased frequency of galaxy-galaxy interactions among members of a group, compared to the interaction rate between isolated galaxies, could be driving the creation of passive spirals in the cluster outskirts. We note that, at the group scale, the effects of impulsive galaxy-galaxy interactions are difficult to separate from galaxy-galaxy tidal interactions that act over a longer timescale, and so we consider them together here. While galaxy-galaxy harassment at the typical velocity dispersions of bound groups has not been widely studied, there are some advantages to this explanation. First, on a larger cluster scale, simulations indicate that harassment of massive cluster spirals results in gas being funneled to the central bulge (Moore et al. 1999), providing a natural mechanism to accelerate star formation and deplete a spiral's gas supply; a similar gas funneling effect due to tidal effects during group preprocessing has also been proposed (e.g., Mihos 2004).

While simulations would be necessary to test the hypothesis, one could imagine a "gentle harassment" mechanism that induces a transport of gas to the galaxy center without immediately destroying the spiral arms. A slow group-scale harassment could possibly reproduce the timescales for quenching of star formation indicated by the starvation model tracks in Figure 6. We note that the timescale for final conversion to S0 morphology may be different from the timescale under starvation and could provide an important discriminator between the two possibilities in the future.

Depending on the rate of gas transport, it is possible that a brief increase in SFR could be detected before the final quenching (Fujita 1998; Kodama & Smail 2001), and this could provide another way to distinguish between this mechanism and starvation. However, within the uncertainties, we cannot confirm any small starbursts among galaxies within infalling groups in our sample. Dividing our total sample of star-forming galaxies by radius into three equally sized bins, we do not see evidence for an enhancement of either the mean or median  $[\text{O II}]$  of a star-forming galaxy in any of the three radial zones. Nor do we see any change in the fraction of star-forming galaxies with strong ( $< -20 \text{ \AA}$ )  $[\text{O II}]$ . However, as the expected lifetime for a burst is short (Fujita 2004), we cannot rule out the presence of small bursts that change the median specific SFR by less than 20%.

A definitive distinction between gas-related processes and galaxy interactions therefore remains elusive. Importantly, however, we have already established that galaxy-galaxy harassment is affecting spirals across both clusters, and at a level that does not destroy their spiral structure: Moran et al. (2007) found that the high scatter in the cluster TF relation compared to the field was most readily understood if galaxy harassment is acting to perturb the kinematics of spirals. Moran et al. (2007) also observed a strange deficit in the cluster outskirts of spirals with high central mass concentrations; one possible explanation is that these galaxies have dropped out of our emission-line sample as they become passive due to the aforementioned funneling of gas to their centers.

While hardly a settled issue, we expect that the action of harassment is more likely to be at the root of the galaxy evolution in

infalling groups, as the mechanism is already known to be acting in Cl 0024 and MS 0451. Yet some contribution from the intra-group gas is also possible, and the two effects could act in combination. Future study of the bulges of spirals and S0s could help distinguish between the mechanisms by establishing whether significant mass has been funneled to centers of galaxies during their evolution, as predicted in the case of harassment.

### 7.2. The Cluster Cores

We turn now to the cores of both clusters, where spirals in MS 0451 appear to have their star formation quenched at a more rapid pace than in Cl 0024. The most obvious explanation for the accelerated truncation of star formation within the central region of MS 0451 is, of course, its much denser ICM. As we saw in Figure 10, rapid truncation of star formation appears to occur in both clusters only in regimes where the ram pressure is high. Due to the dense ICM in MS 0451, such an environment is much more widespread in this cluster, and so, unlike in Cl 0024, most of the passive spirals in its core are experiencing a rapid truncation of star formation.

Ram pressure stripping, in regimes where it is effective, can strip an entire spiral disk in less than 100 Myr (Quilis et al. 2000; Fujita & Nagashima 1999). Detailed analysis of local analogs of passive spirals thought to be undergoing ram pressure stripping suggests a timescale of  $\sim 300$  Myr for the process to produce a galaxy similar to the UV-undetected passive spirals we observe (Boselli et al. 2006; Cortese et al. 2007). Both of these are consistent with the maximum timescale of 400 Myr implied by the 600 kpc hole devoid of spirals at the center of MS 0451. Further, there is some evidence that poststarburst/post-star-forming galaxies in the Coma Cluster, similar to but fainter than those in MS 0451, are generated via ram pressure stripping (Poggianti et al. 2004).

The fact that we observe passive spirals at all implies that the transformation to S0 is not precisely simultaneous with the halt in star formation (Poggianti et al. 1999). However, the truncated star formation history models presented in Figure 6 suggest that  $D_n(4000)$  strength will increase at a fast rate after truncation, such that we must be seeing young S0s within 100 Myr of the halt in star formation. The similar fraction of galaxies observed in both the passive spiral phase and the young S0 phase supports the idea that the lifetimes for each phase are comparable, at about 100 Myr.

Yet there are several remaining uncertainties in this simple picture. Ram pressure stripping alone does not alter disk kinematics and spiral structure on such a short timescale, so there must be an additional mechanism to speed the conversion. In the cluster cores, harassment and/or tidal interactions could provide this additional impetus (e.g., Cortese et al. 2007; Mihos 2004). In Cl 0024, in the absence of rapid truncation by the ICM, a similar harassment or tidal process must be at work. However, the complex substructure of Cl 0024, and particularly the effects of the recent cluster collision, may generate important differences between the two clusters.

In order to better constrain the mechanisms affecting passive spirals in the cores of Cl 0024 and MS 0451, we are aided by two supplementary observations, one of which illuminates the action of harassment, with the other providing further constraints on ICM interactions, particularly the hypothesis that shocks in the ICM could be important.

#### 7.2.1. Compact Emission-Line Ellipticals

As discussed in § 2, we found in Cl 0024 a population of relatively faint elliptical galaxies with strong emission, concentrated

in a narrow range in radius close to the virial radius. We cast doubt on the idea that major mergers were the cause of these apparent starbursts, and we speculated that another rapidly acting physical interaction must be triggering these bursts of activity. Strong shocks in the ICM of Cl 0024 could easily have been generated (Roettiger et al. 1996) during the cluster-subcluster merger (Czoske et al. 2002), and these shocks could be responsible for the triggered starbursts/AGNs we observe.

If this were the case, we hypothesized that we would not see such bursts in MS 0451, as its smoother large-scale structure makes it less likely that such shocks would be generated. Referring back to Figure 9, however, we see that objects of this type are indeed found in the outskirts of both clusters. While only half as many are identified in MS 0451 as in Cl 0024, this detection rate is consistent with the lower spectroscopic completeness of our MS 0451 campaign for galaxies at these low luminosities: in MS 0451, 10% of detected cluster members are at  $M_V \geq 19.6$ , while in Cl 0024, the fraction is 20%.

The properties of these objects, compact size,  $[O II] < -15 \text{ \AA}$ , and typical luminosities  $M_V = -19.2$ , associate them with a class of objects dubbed CNELGs (Koo et al. 1995), or their more luminous cousins the luminous blue compact galaxies (LBCGs; e.g., Noeske et al. 2006). Analysis by Rawat et al. (2007) of deep ACS imaging of LBCGs reveals that more than  $\frac{1}{3}$  show signs of a recent merger. Their positions outside of dense regions in both MS 0451 and Cl 0024 support the notion that these galaxies may simply represent the remnants of a merger between small, gas-rich galaxies.

In this interpretation, two important constraints can be put on the physical processes acting on passive spirals. First, we have eliminated the possibility that strong shocks in the Cl 0024 ICM have a significant effect, even on low-mass galaxies. Secondly, the minimum cluster radii at which these CNELGs/LBCGs are found identify empirically the point at which merging becomes impossible and harassment must begin to dominate any galaxy-galaxy interaction.

In Cl 0024 this occurs nearly at the virial radius, while in MS 0451 it occurs at a similar projected radius of 1.5 Mpc. We expect, then, that harassment within 1.5 Mpc should scale in strength similarly between the two clusters. If harassment is responsible for the slow conversion of spirals to S0s in the Cl 0024 core, it should also be acting on MS 0451 spirals with similar strength.

#### 7.2.2. Fundamental Plane

An analysis of the FP can provide sensitive constraints on the star formation and kinematic histories of E+S0s (Paper III). In Cl 0024, we observed that elliptical and S0 galaxies form a clear FP (Fig. 11), yet they exhibit a high scatter, equivalent to a spread of 40% in mass-to-light ratio ( $M/L_V$ ).<sup>8</sup> On closer inspection, this high scatter appeared to occur only among galaxies within 1 Mpc of the cluster core. We suggested in Paper III that the enhanced scatter in the cluster core may somehow be related to the recent cluster-subcluster merger in Cl 0024 (Czoske et al. 2002). By examining the FP and its residuals for MS 0451 as well, we can test the hypothesis that galaxy interactions in the core of Cl 0024 are enhanced over that expected for a relaxed cluster.

In constructing the FP for both clusters, surface brightness ( $\mu_V$ ) and effective radius ( $R_e$ ) are determined via the GALFIT

<sup>8</sup> As discussed in Paper III, a galaxy's deviation from the FP can be thought of as a change in mass-to-light ratio, via the relation  $\Delta \log(M/L_V) = \Delta \gamma / (2.5\beta)$ , where  $\beta$  is the slope of the FP and  $\Delta \gamma$  is each galaxy's deviation from the cluster's overall FP intercept  $\gamma$ .

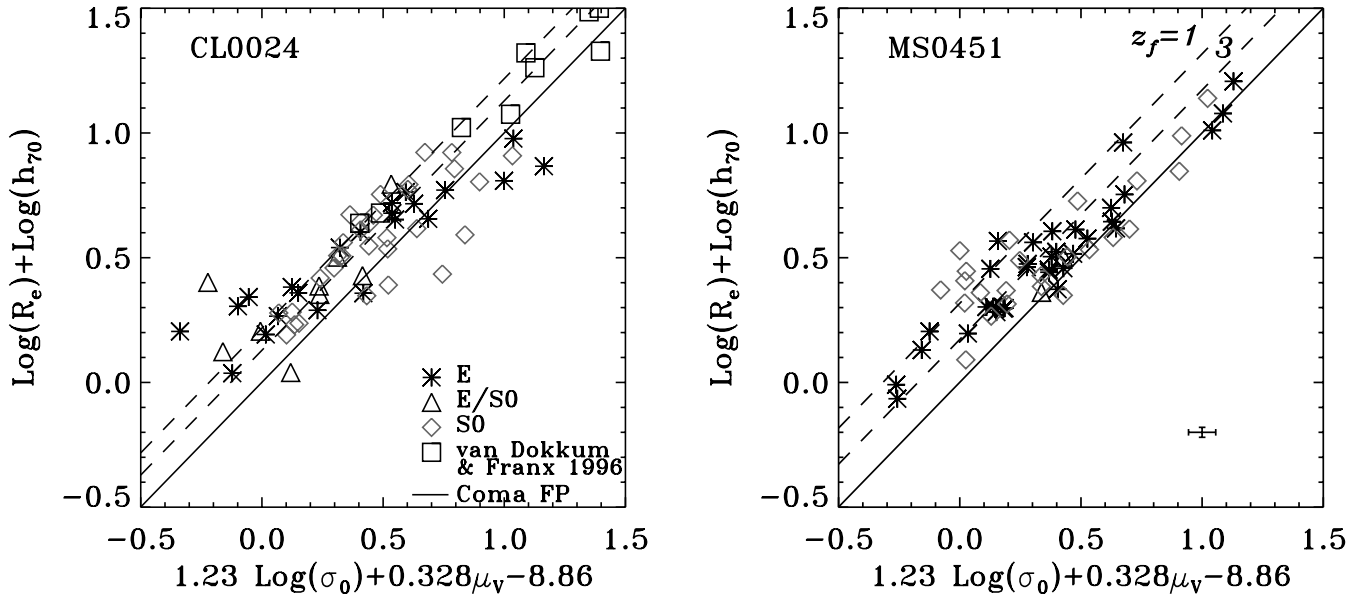


FIG. 11.—FP of E+S0s in MS 0451 (left) and CI 0024 (right). Symbols represent different morphologies, as indicated in the legend. The solid line is the local FP for the Coma Cluster, adapted from Lucey et al. (1991). Dashed lines indicate the expected positions for early types that formed in a single burst at  $z = 1$  or  $3$ , calculated according to the models of Bruzual & Charlot (2003). A typical error bar is shown in the lower right of the MS 0451 panel. [See the electronic edition of the Journal for a color version of this figure.]

software (Peng et al. 2002), which fits a two-dimensional model to the *HST* imaging. We fit models following the de Vaucouleur’s function to each galaxy (see Paper III) and apply a  $k$ -correction from observed F814W magnitudes to rest-frame  $V$ -band surface brightness,  $\mu_V$ , as discussed in § 3.

The resulting FP for our sample of 60 E+S0 galaxies in MS 0451 is shown in Figure 11, alongside the previously published FP for CI 0024. For both CI 0024 and MS 0451, we overplot the local FP from the Coma Cluster (Lucey et al. 1991) as a solid line, adapted to our chosen cosmology. In addition, we plot two parallel dashed lines indicating the galaxies’ expected FP intercept if they had formed in a single burst at  $z_f = 1$  or  $3$ , calculated using the Bruzual & Charlot (2003) models. It is clear that the E+S0 populations in both clusters have largely formed their stars at  $z > 1$ . Nevertheless, the high scatter in the CI 0024 FP also seems to be present in MS 0451. Limiting our sample to those galaxies with  $\sigma > 100 \text{ km s}^{-1}$  as in Paper III, the overall scatter is  $0.18 \pm 0.02$ , expressed in terms of a spread in  $\log(M/L_V)$ , compared to  $0.16 \pm 0.02$  for CI 0024.

A small portion of this large scatter in  $M/L_V$  can be attributed to the higher redshift of MS 0451, where an equivalent spread in galaxy formation ages translates into a larger FP scatter at  $z = 0.54$  than at  $z = 0.4$ . In Figure 11, this effect is most easily seen by noting the larger separation between the  $z_f = 1$  and  $3$  model lines in the MS 0451 panel, compared to the CI 0024 panel. If MS 0451 early types were to passively evolve between  $z = 0.54$  and  $0.4$ , the single stellar population (SSP) models of Bruzual & Charlot (2003) predict a decrease in the FP scatter of only up to  $\sim 0.04$ .

This still leaves an unexpectedly large spread in mass-to-light ratios for MS 0451 early types. In Figure 12 we plot each galaxy’s residual from the FP as a function of its dynamical mass, calculated according to  $M = 5\sigma^2 R_e / G$  (see Paper III). In both clusters, we observe a clear “downsizing” trend that has been described by several authors (e.g., Treu et al. 2005), the tendency for less massive E+S0s to exhibit lower mass-to-light ratios, implying younger stellar populations.

To judge the effects of downsizing, we fit a straight line to the FP residuals as a function of mass, limiting the fit to masses above

$5 \times 10^{10} M_\odot$ , where selection effects are minimal. In MS 0451, subtracting off this extra “tilt” to the FP greatly tightens the observed scatter, to  $\Delta \log(M/L_V) = 0.12$ , a level of scatter consistent with that of other well-virialized clusters at lower redshift (e.g., Kelson et al. 2000).

Performing the same exercise on CI 0024, however, results in no improvement in the FP scatter. Close inspection of the morphologies of galaxies in Figure 12 uncovers the reason. While ellipticals in CI 0024 display a tight sequence in mass, S0s, especially at intermediate masses of  $\sim 10^{11} M_\odot$ , exhibit a remarkable scatter in their FP residuals. These residuals do not appear to correlate with any typical measures of SFR or mass-to-light ratio, including  $D_n(4000)$ ,  $H\delta_A$ , or even broadband optical colors. It seems, then, that the previously described FP scatter in the core of CI 0024 can be ascribed almost entirely to S0s whose properties do not obey any simple trends with mass or star formation.

Furthermore, a significant number of CI 0024 galaxies exhibit FP residuals  $\Delta \log(M/L_V) > 0$ , an unphysical quantity that either indicates stellar populations older than those of Coma Cluster early types (impossible due to the much younger age of the universe at  $z = 0.4$  and the extreme mass-to-light ratios implied) or else indicates the breakdown of the FP for these objects. In contrast, all of the scatter in MS 0451 early types is in the expected direction, in the sense that some galaxies have younger stellar populations with  $\Delta \log(M/L_V) < 0$ , while the most massive ellipticals and S0s lie neatly on the local FP.

What could be generating these abnormal galaxies in CI 0024 but not in MS 0451? Enhanced levels of galaxy-galaxy interaction due to the complex substructure in CI 0024 are the most likely explanation. The difference between a slow conversion of spirals to S0s (in CI 0024) and a rapid truncation of star formation (in MS 0451) could also affect the positions of S0s on the FP. Future simulations to test this possibility would be welcome. We note that the actual young S0s are only sparsely represented in Figure 12, due to the smaller sample of galaxies that can be plotted on the FP, and are not driving the observed difference by themselves.

What, then, are the implications for the physical processes driving galaxy evolution in the cores of both clusters? In short,

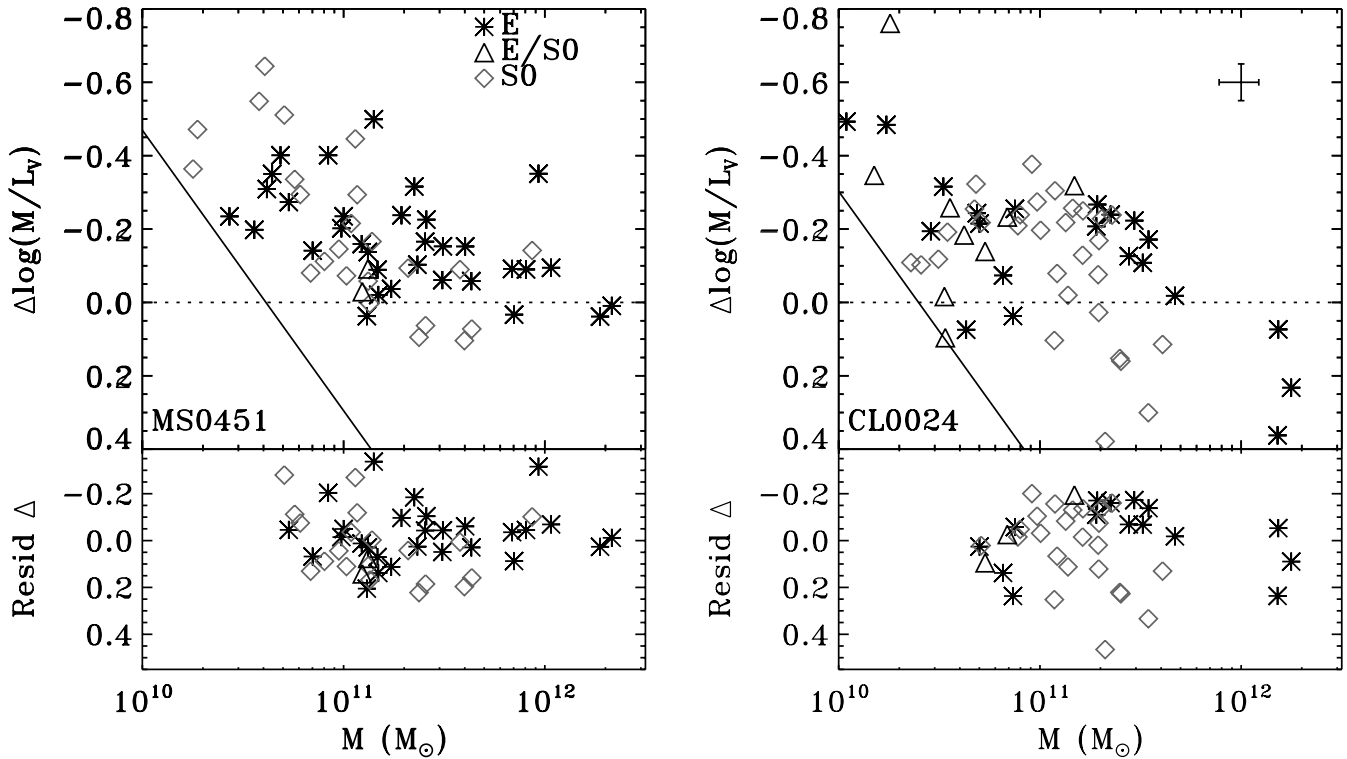


FIG. 12.—The  $\Delta \log(M/L_V)$  vs. dynamical mass,  $M$ , for MS 0451 (left) and CL 0024 (right). Symbols denote different morphologies as indicated in the legend. We are insensitive to galaxies in the area to the lower left of each solid black line, due to the luminosity limit of our sample. Above  $\sim 5 \times 10^{10} M_\odot$ , we are nearly unbiased. Lower split panels show the residuals from fitting and subtracting a straight line to galaxies at  $M > 5 \times 10^{10} M_\odot$ . The  $\Delta \log(M/L_V)$  for S0s in CL 0024 do not form a tight sequence in mass, while their counterparts in MS 0451 and the Es in both clusters do form a tight sequence. Many CL 0024 galaxies also occupy unphysical locations at  $\Delta \log(M/L_V) > 0$ . [See the electronic edition of the *Journal* for a color version of this figure.]

we can conclude that the complex recent assembly history of CL 0024 *does not* enhance the ability of the ICM to transform galaxies via shocks, but it *does* appear to enhance the observed kinematic disturbance of galaxies within the cluster core. Some mix of galaxy-galaxy interaction and tidal interaction therefore must dominate in the core of CL 0024, driving the steady decline in SFR within its spiral population. Only for galaxies that reach the inner  $\sim 300$  kpc will ram pressure stripping become important.

In contrast, the quenching of star formation in MS 0451 is almost certainly driven by ram pressure from the ICM, probably coupled with galaxy and tidal interactions that serve to erase spiral structure and complete the morphological conversion. In MS 0451, the effects of harassment/tidal interaction must complete the morphological conversion more rapidly than in CL 0024, where the stellar populations of passive spirals indicate that they are long lived ( $\sim 1-2$  Gyr). At the same time, the effects of this conversion must somehow decay rapidly enough in MS 0451 S0s to be unobserved in the residuals from the FP. Future investigations into the effects of harassment on the S0 FP could help shed light on this issue.

## 8. DISCUSSION AND CONCLUSIONS

In this paper we have presented new results from our comprehensive comparative survey of two massive, intermediate-redshift galaxy clusters, CL 0024+17 ( $z = 0.39$ ) and MS 0451-03 ( $z = 0.54$ ). We have identified and studied several key classes of transition objects in the clusters: the passive spirals and the young S0s. Through UV imaging and measurements of spectral line indices, we have concluded that some passive spirals have experienced a decline in star formation over a  $\sim 1$  Gyr timescale, mostly in CL 0024, while others, mostly in MS 0451, have ex-

perienced a more rapid truncation in star formation. For the first time, we have been able to conclusively identify spiral galaxies in the process of transforming into S0 galaxies, by directly linking the passive spirals in each cluster with their descendant S0s.

Having established that the transformation from spiral to S0 galaxies is taking place in each cluster, we have leveraged the differences between clusters in the timescales and spatial location of the conversion process, in order to evaluate the relative importance of several proposed physical mechanisms that could be responsible for the transformation. Combined with other diagnostics that are sensitive to either ICM-driven galaxy evolution or galaxy-galaxy interactions, including the residuals from the FP and the properties of signpost compact emission-line galaxies, we paint a tentative but remarkably self-consistent picture of galaxy evolution in clusters.

We find that spiral galaxies within infalling groups have already begun a slow process of conversion into S0s primarily via gentle galaxy-galaxy interactions that act to quench star formation, perhaps aided by interaction with the intragroup gas. The fates of spirals on reaching the core of the cluster depend heavily on the cluster ICM, with rapid conversion of all remaining spirals into S0s via ram pressure stripping in clusters where the pressure of the ICM is  $\geq 20\%$  of that needed to strip a canonical Milky Way-like spiral. In the presence of a less dense ICM, the conversion continues at a slower pace, with galaxy-galaxy interactions continuing to play a role, perhaps along with starvation or gentle stripping by the ICM.

Several authors have raised objections to a scenario where S0s are created via simple fading of spiral disks. First, S0s are observed to have higher bulge-to-disk ratios than their supposed spiral progenitors (e.g., Burstein et al. 2005), suggesting that if

the spiral-to-S0 conversion takes place, significant redistribution of mass or significant new star formation is required (Christlein & Zabludoff 2004; Kodama & Smail 2001). Second, other authors have noted that the local abundance of S0s is only weakly correlated with environment, such that processes like ram pressure stripping that act only in cluster cores cannot be responsible for the entire buildup of S0s (Dressler 1980, 2004).

We have here demonstrated, however, that simple stripping of gas does *not* build up the entire population of cluster S0s. Rather, a combination of gas effects and galaxy interactions is responsible, in ratios that vary widely and depend on both the cluster dynamical state and the location within the cluster or its outskirts. The buildup of bulges through new star formation (Christlein & Zabludoff 2004) that is expected from harassment-like encounters could potentially balance out the expected fading of disks after ram pressure stripping has run its course. It may still be necessary to invoke significant obscured star formation to bridge the observed gap between the bulges of spirals and S0s (Kodama & Smail 2001); the higher detection rate of such systems in Cl 0024 compared to MS 0451 (Geach et al. 2006) may indicate that such obscured starbursts are part of the preprocessing that occurs before galaxies encounter a dense ICM.

Furthermore, the wide distribution of passive spirals across both clusters, as well as their association with groups in the cluster outskirts, indicates that the resulting S0s will likely be spread across a wide range of environments. The typical densities of infalling groups at  $z \sim 0.5$  are likely realized even in isolated groups by  $z = 0$  (Fujita 2004), and so it seems that, although a variety of mechanisms are responsible, passive spirals could be the progenitors of most local S0s.

In Moran et al. (2006) a rough assessment of the frequency of passive spirals and their expected lifetimes in Cl 0024 suggested that passive spirals could account for the entire buildup of S0s between  $z = 0.4$  and 0. In MS 0451, we observe a similar number of spirals currently in the passive phase, but we have shown that the timescale for conversion is much shorter than in Cl 0024. This suggests that all existing spirals should be converted to S0 in MS 0451 even *before*  $z = 0$ , and the rate of any future buildup should be limited by the infall rate of new galaxies. As MS 0451 is a remarkably well evolved system at  $z = 0.54$ , comparable in mass to Virgo or Coma ( $6.9 \times 10^{14}$  and  $1.1 \times 10^{15} M_{\odot}$ , respectively; Biviano et al. 1991; Fouqué et al. 2001; Geller et al. 1999), this is perhaps not surprising.

It suggests, however, that there may exist a generic tipping point in the evolution of a massive cluster: beyond the threshold in ram pressure strength that we have identified here (which is reached through some combination of cluster mass and ICM density), spirals are transformed so rapidly on infall that they will be essentially absent. By  $z = 0$ , many clusters have likely reached this threshold, as evidenced by their low spiral fractions (Dressler et al. 1997; Dressler 1980). This sort of dichotomy between well-evolved and still-assembling clusters could, for example, explain why some clusters, like Coma, reveal few signs of evolution in their massive galaxies (Poggianti et al. 2004), while others, like Virgo, have a rich population of passive spirals and galaxies with other signs of recent evolution (e.g., Chung et al. 2007).

Regardless, the results presented here indicate that the abundant cluster spirals found at intermediate redshift *do*, in fact, transform into the equally abundant S0 population seen today. The transformation process at  $z = 0.5$ , as we have seen, is beginning to operate even in groups at the cluster outskirts. As a result, the conversion of passive spirals to S0s can account for the evolution of the morphology-density relation at both the cluster and group scale from intermediate redshift to today.

We thank the referee, A. Boselli, for insightful comments, especially on the various physical processes and their timescales, which were helpful in revising the discussion of these issues. S. M. M. would like to thank T. Heckman, G. Kauffmann, S. Yi, and members of the *GALEX* science team for valuable discussions. Faint object spectroscopy at Keck Observatory is made possible with LRIS and DEIMOS thanks to the dedicated efforts of J. Cohen, P. Amico, S. Faber, and G. Wirth. We acknowledge use of the Gauss-Hermite Pixel Fitting Software developed by R. P. van der Marel. The analysis pipeline used to reduce the DEIMOS data was developed at UC Berkeley with support from NSF grant AST 00-71048. T. T. acknowledges support from the NSF through CAREER award NSF-0642621 and from the Sloan Foundation through a Sloan Research Fellowship. R. S. E. acknowledges financial support from NSF grant AST 03-07859 and STScI grants HST-GO-08559.01-A and HST-GO-09836.01-A. Finally, I. R. S. and G. P. S. acknowledge support from the Royal Society.

#### REFERENCES

- Abraham, R. G., et al. 1996, *ApJ*, 471, 694  
 Balogh, M. L., Morris, S. L., Yee, H. K. C., Carlberg, R. G., & Ellingson, E. 1999, *ApJ*, 527, 54  
 Bekki, K., Couch, W. J., & Shioya, Y. 2002, *ApJ*, 577, 651  
 Bertin, E., & Arnouts, S. 1996, *A&AS*, 117, 393  
 Biviano, A., Girardi, M., Giuricin, G., Mardirossian, F., & Mezzetti, M. 1991, *ApJ*, 376, 458  
 Blanton, M. R., et al. 2003, *AJ*, 125, 2348  
 Boselli, A., Boissier, S., Cortese, S., Gil de Paz, A., Seibert, M., Madore, B. F., Buat, V., & Martin, D. C. 2006, *ApJ*, 651, 811  
 Boselli, A., & Gavazzi, G. 2006, *PASP*, 118, 517  
 Bruzual, G., & Charlot, S. 2003, *MNRAS*, 344, 1000  
 Burstein, D., Ho, L. C., Huchra, J. P., & Macri, L. M. 2005, *ApJ*, 621, 246  
 Christlein, D., & Zabludoff, A. I. 2004, *ApJ*, 616, 192  
 Chung, A., van Gorkom, J. H., Kenney, J. D. P., & Vollmer, B. 2007, *ApJ*, 659, L115  
 Cooper, M. C., et al. 2007, *MNRAS*, 376, 1445  
 Cortese, L., et al. 2007, *MNRAS*, 376, 157  
 Couch, W. J., Barger, A. J., Smail, I., Ellis, R. S., & Sharples, R. M. 1998, *ApJ*, 497, 188  
 Cowie, L. L., & Songaila, A. 1977, *Nature*, 266, 501  
 Czoske, O., Kneib, J.-P., Soucail, G., Bridges, T. J., Mellier, Y., & Cuillandre, J.-C. 2001, *A&A*, 372, 391  
 Czoske, O., Moore, B., Kneib, J.-P., & Soucail, G. 2002, *A&A*, 386, 31  
 Davis, M., et al. 2003, *Proc. SPIE*, 4834, 161  
 De Filippis, E., Sereno, M., Bautz, M., & Longo, G. 2005, *ApJ*, 625, 108  
 de Lucia, G., Springel, V., White, S. D., Croton, D., & Kauffmann, G. 2006, *MNRAS*, 366, 499  
 Donahue, M., Gaskin, J. A., Patel, S. K., Joy, M., Clowe, D., & Hughes, J. P. 2003, *ApJ*, 598, 190  
 Dressler, A. 1980, *ApJ*, 236, 351  
 ———. 2004, in *Clusters of Galaxies: Probes of Cosmological Structure and Galaxy Evolution*, ed. J. S. Mulchaey, A. Dressler, & A. Oemler (Cambridge: Cambridge Univ. Press), 206  
 Dressler, A., & Shectman, S. A. 1988, *AJ*, 95, 985  
 Dressler, A., Smail, I., Poggianti, B., Butcher, H., Couch, W. J., Ellis, R. S., & Oemler, A., Jr. 1999, *ApJS*, 122, 51  
 Dressler, A., et al. 1997, *ApJ*, 490, 577  
 Ellingson, E., Yee, H. K. C., Abraham, R. G., Morris, S. L., & Carlberg, R. G. 1998, *ApJS*, 116, 247  
 Fouqué, P., Solanes, J. M., Sanchis, T., & Balkowski, C. 2001, *A&A*, 375, 770  
 Fujita, Y. 1998, *ApJ*, 509, 587  
 ———. 2004, *PASJ*, 56, 29  
 Fujita, Y., & Nagashima, M. 1999, *ApJ*, 516, 619  
 Gavazzi, G., Boselli, A., Cortese, L., Arosio, I., Gallazzi, A., Pedotti, P., & Carrasco, L. 2006, *A&A*, 446, 839

- Gavazzi, G., Zaccardo, A., Sanvito, G., Boselli, A., & Bonfanti, C. 2004, *A&A*, 417, 499
- Geach, J. E., et al. 2006, *ApJ*, 649, 661
- Geller, M. J., Diaferio, A., & Kurtz, M. J. 1999, *ApJ*, 517, L23
- Gunn, J. E., & Gott, J. R. 1972, *ApJ*, 176, 1
- Hester, J. A. 2006, *ApJ*, 647, 910
- Jee, M. J., et al. 2007, *ApJ*, 661, 728
- Jeltema, T. E., Mulchaey, J. S., Lubin, L. M., & Fassnacht, C. D. 2007, *ApJ*, 658, 865
- Kauffmann, G., et al. 2003, *MNRAS*, 341, 33
- Kelson, D. D., Illingworth, G. D., van Dokkum, P. G., & Franx, M. 2000, *ApJ*, 531, 184
- Kneib, J.-P., et al. 2003, *ApJ*, 598, 804 (Paper II)
- Kodama, T., & Smail, I. 2001, *MNRAS*, 326, 637
- Koo, D., Guzmán, R., Faber, S. M., Illingworth, G. D., Bershad, M. A., Kron, R. G., & Takamiya, M. 1995, *ApJ*, 440, L49
- Larson, R. B., Tinsley, B. M., & Caldwell, C. N. 1980, *ApJ*, 237, 692
- Lucey, J. R., Guzmán, R., Carter, D., & Terlevich, R. J. 1991, *MNRAS*, 253, 584
- Martin, D. C., et al. 2005, *ApJ*, 619, L1
- Mihos, J. C. 2004, in *IAU Symp. 217, Recycling Interstellar and Intergalactic Matter*, ed. P.-A. Duc, J. Braine, & E. Brinks (San Francisco: ASP), 390
- Moore, B., Lake, G., Quinn, T., & Stadel, J. 1999, *MNRAS*, 304, 465
- Moran, S. M., Ellis, R. S., Treu, T., Salim, S., Rich, R. M., Smith, G. P., & Kneib, J.-P. 2006, *ApJ*, 641, L97
- Moran, S. M., Ellis, R. S., Treu, T., Smail, I., Dressler, A., Coil, A. L., & Smith, G. P. 2005, *ApJ*, 634, 977 (Paper III)
- Moran, S. M., Miller, N., Treu, T., Ellis, R. S., & Smith, G. P. 2007, *ApJ*, 659, 1138
- Mulchaey, J. 2000, *ARA&A*, 38, 289
- Noeske, K. G., Koo, D. C., Phillips, A. C., Willmer, C. N. A., Melbourne, J., de Paz, A. G., & Papaderos, P. 2006, *ApJ*, 640, L143
- Nulsen, P. E. J. 1982, *MNRAS*, 198, 1007
- Okamoto, T., & Nagashima, M. 2003, *ApJ*, 587, 500
- Ota, N., Pointecouteau, E., Hattori, M., & Mitsuda, K. 2004, *ApJ*, 601, 120
- Peng, C. Y., Ho, L. C., Impey, C. D., & Rix, H. 2002, *AJ*, 124, 266
- Poggianti, B. M., & Barbaro, G. 1996, *A&A*, 314, 379
- . 1997, *A&A*, 325, 1025
- Poggianti, B. M., Bridges, T. J., Komiyama, Y., Yagi, M., Carter, D., Mobasher, B., Okamura, S., & Kashikawa, N. 2004, *ApJ*, 601, 197
- Poggianti, B. M., Smail, I., Dressler, A., Couch, W. J., Barger, A. J., Butcher, H., Ellis, R. S., & Oemler, A., Jr. 1999, *ApJ*, 518, 576
- Poggianti, B. M., et al. 2001, *ApJ*, 563, 118
- . 2006, *ApJ*, 642, 188
- Postman, M., et al. 2005, *ApJ*, 623, 721
- Quilis, V., Moore, B., & Bower, R. 2000, *Science*, 288, 1617
- Rawat, A., Kembhavi, A. K., Hammer, F., Flores, H., & Barway, S. 2007, *A&A*, 469, 483
- Roettiger, K., Burns, J., & Loken, C. 1996, *ApJ*, 473, 651
- Schlegel, D. J., Finkbeiner, D. P., & Davis, M. 1998, *ApJ*, 500, 525
- Smith, G. P., Treu, T., Ellis, R. S., Moran, S. M., & Dressler, A. 2005a, *ApJ*, 620, 78
- Smith, G. P., et al. 2005b, *MNRAS*, 359, 417
- Treu, T., Ellis, R. S., Kneib, J.-P., Dressler, A., Smail, I., Czoske, O., Oemler, A., & Natarajan, P. 2003, *ApJ*, 591, 53 (Paper I)
- Treu, T., et al. 2005, *ApJ*, 633, 174
- van den Bergh, S. 1976, *ApJ*, 206, 883
- van der Marel, R. 1994, *MNRAS*, 270, 271
- Wilson, J. C., et al. 2003, *Proc. SPIE*, 4841, 451
- Worthey, G., Faber, S. M., Gonzalez, J. J., & Burstein, D. 1994, *ApJS*, 94, 687
- Zabludoff, A., & Mulchaey, J. 1998, *ApJ*, 496, 39
- Zhang, Y.-Y., Böhringer, H., Mellier, Y., Soucail, G., & Forman, W. 2005, *A&A*, 429, 85